Studies on the overexpression of antimicrobial peptides in *E. coli*

（大腸菌を用いた抗菌ペプチドの大量生産に関する研究）

Graduate School of Life Science

Hokkaido University

2015

Satoshi Tomisawa

Contents

General Introduction

Antimicrobial peptides play an important role in innate immunity as a part of the host defense response [1,2]. Most antimicrobial peptides contain a net positive charge which could be important for the interaction with the negatively charged bacterial cell membrane. Antimicrobial peptides are thought to kill bacteria by breaking their cell membranes, although the exact mechanisms are still unclear [3,4]. To date, numerous antimicrobial peptides have been identified in a wide range of organisms, such as mammals, insects, and plants [5].

Large quantities of correctly folded antimicrobial peptide are essential to study the structure and antimicrobial activity. In general, it is difficult to obtain large amounts of antimicrobial peptides from natural sources due to their low concentration in these materials. Although chemically synthesized antimicrobial peptides were widely used in some previous studies [6-8], the chemical synthesis of antimicrobial peptide is very costly. Therefore, many strategies have been developed to produce antimicrobial peptide using recombinant techniques [9-13]. Because *E. coli* is easy to handle, is inexpensive, and grows quite fast, *E. coli* is the most widely used host strain for the overproduction of antimicrobial peptide [11-13]. However, the recombinant production of antimicrobial peptide using *E. coli* has been difficult due to their toxicity and proteolytic susceptibility. The formation of inclusion bodies may be useful to avoid toxicity and proteolytic degradation of antimicrobial peptides. However, it is difficult to control inclusion body formation in *E. coli* cells.

In Chapter 1, therefore, I applied a coexpression method for the production of ABF-2 (antibacterial factor 2) to enhance inclusion body formation. In this method, it is expected that coexpression of the aggregation-prone protein (partner protein) enhances the inclusion body formation of the peptide of interest (target peptide) and protects the target peptide

from proteolytic degradation by protease. Moreover, I evaluated the effect of the charge of partner proteins on inclusion body formation of ABF-2 in this method by using four structurally homologous proteins. I concluded that the opposite charge of a partner protein enhanced the formation of an inclusion body of the target peptide efficiently.

In Chapter 2, I applied the coexpression method to produce mouse α-defensin Crp4 (cryptdin-4) in order to enhance the inclusion body formation. Moreover, I attempted to refold Crp4 directly during the inclusion-body solubilization step under oxidative conditions. Interestingly, even without any purification, Crp4 was efficiently refolded in the solubilization step, and the yield was better than that by the conventional refolding method.

In Chapter 3, I show that the previously developed vacuum-assisted detection method greatly improves the detection of small peptides without additional protocol modification. Western blotting is a widely used technique for the detection and quantification of proteins and peptides. However, it is challenging to detect small peptides, such as antimicrobial peptides, efficiently by the conventional Western blotting method with shaking, in part because the peptides readily detach from the blotted membrane. Although some modified Western blotting protocols have been developed to overcome this problem [14-16], it remains difficult to prevent peptide detachment from the membrane. The vacuum-assisted method was developed to shorten the time required for all immunodetection steps, and all the Western blotting solutions penetrated the membrane quickly and efficiently by this method. By using this vacuum method, I succeeded in detecting peptides that were completely undetectable by the conventional Western blotting method.

References

[1] T. Gnaz, The role of antimicrobial peptides in innate immunity, Integr. Comp. Biol. 43 (2003) 300-304.

[2] K. Radek, R. Gallo, Antimicrobial peptides: natural effectors of the innate immune system, Semin. Immunol. 29 (2007) 27-43.

[3] H. Sato, J.B. Feix, Peptide-membrane interactions and mechanisms of membrane destruction by amphipathic α-helical antimicrobial peptides, Biochim. Biophys. Acta. 1758 (2006) 1245-1256.

[4] R. Mani, A.J. Waring, R.I. Lehrer, M. Hong, Membrane-disruptive abilities of beta-hairpin antimicrobial peptides correlate with conformation and activity: a 31P and 1H NMR study, Biochim. Biophys. Acta. 1716 (2005) 11-18.

[5] M. Zasloff, Antimicrobial peptides of multicellular organisms, Nature 415 (2002) 389-395.

[6] Z. Wu, B. Ericksen, K. Tucker, J. Lubkowski, W. Lu, Synthesis and characterization of human α-defensins 4-6, J. Pept. Res. 64 (2004) 118-125.

[7] L. Carlier, P. Joanne, L. Khemtémourian, C. Lacombe, P. Nicolas, C. El Amri, O. Lequin, nvestigating the role of GXXXG motifs in helical folding and self-association of plasticins, Gly/Leu-rich antimicrobial peptides, Biophys. Chem. 196 (2015) 40-52.

[8] CS. Lee, WC. Tung, YH. Lin, Deletion of the carboxyl-terminal residue disrupts the

amino-terminal folding, self-association, and thermal stability of an amphipathic antimicrobial peptide, J. Pept. Sci. 20 (2014) 438-445.

[9] F.L. Jin, X.X. Xu, W.Q. Zhang, D.X. Gu, Expression and characterization of a housefly cecropin gene in the methylotrophic yeast, *Pichia pastoris*, Protein Expr. Purif., 49 (2006) 39–46.

[10] D. Destoumieux, P. Bulet, J.M. Strub, A.V. Dorsellaer, E. Bachère, Recombinant expression and range of activity of penaeidins, antimicrobial peptides from penaeid shrimp, Eur. J. Biochem., 266 (1999) 335-346.

[11] O. Bruhn, P. Regenhard, M. Michalek, S. Paul, C. Gelhaus, S. Jung, G. Thaller, R. Podschun, M. Leippe, J. Grötzinger, E. Kalm, A novel horse α-defensin: gene transcription, recombinant expression and characterization of the structure and function, Biochem. J. 407 (2007) 267-276.

[12] B. Bommarius, H. Jenssen, M. Elliott, J. Kindrachuk, M. Pasupuleti, H. Gieren, K.-E. Jaeger, R.E.W. Hancock, D. Kalman, Cost-effective expression and purification of antimicrobial and host defense peptides in *Escherichia coli*, Peptides 31 (2011) 1957–1965.

[13] L. Xing, W. Xu, B. Zhou, Y. Chen, Z. Lin, Facile expression and purification of the antimicrobial peptide histatin 1 with a cleavable self-aggregating tag (cSAT) in *Escherichia coli*, Protein. Expr. Purif. 88 (2013) 248–253.

[14] N. Nishi, M Inui, H. Miyanaka, H. Oya, F. Wada, Western Blot Analysis of Epidermal

Growth Factor Using Gelatin-Coated Polyvinylidene Difluoride Membranes, Anal. Biochem. 227 (1995) 401-402.

[15] Y. Suzuki, Y. Takeda, T. Ikuta, Immunoblotting conditions for human hemoglobin chains, Anal. Biochem. 378 (2008) 218-220.

[16] B.R. Lee, T. Kamitani, Improved Immunodetection of Endogenous α-Synuclein, PLoS one 6 (2011) e23939.

Chapter 1

Overexpression of an antimicrobial peptide derived from *C. elegans* using an aggregation-prone protein coexpression system

1-1 Abstract

ABF-2 (antibacterial factor 2) is a 67-residue antimicrobial peptide derived from the nematode *Caenorhabditis elegans*. Although it has been reported that ABF-2 exerts in vitro microbicidal activity against a range of bacteria and fungi, the structure of ABF-2 has not yet been solved. To enable structural studies of ABF-2 by NMR spectroscopy, a large amount of isotopically labeled ABF-2 is essential. However, the direct expression of ABF-2 in *Escherichia coli* was difficult to achieve due to its instability. Therefore, I applied a coexpression method to the production of ABF-2 in order to enhance the inclusion body formation of ABF-2. The inclusion body formation of ABF-2 was vastly enhanced by coexpression of aggregation-prone proteins (partner proteins). By using this method, I succeeded in obtaining milligram quantities of active correctly folded ABF-2. In addition, ^{15}N-labeled ABF-2 and a well-dispersed HSQC spectrum were also obtained successfully. Moreover, the effect of the charge of the partner protein on the inclusion body formation of ABF-2 in this method was investigated by using four structurally homologous proteins. I concluded that the opposite charge of a partner protein enhanced the formation of an inclusion body of the target peptide efficiently.

1-2 Introduction

Antimicrobial peptides play an important role in innate immunity as a part of the host defense response [1,2]. Antimicrobial peptides are thought to kill bacteria by breaking their cell membranes, although the exact mechanisms are still unclear [3,4]. To date, numerous antimicrobial peptides have been identified in a wide range of organisms, such as mammals, insects, and plants [5].

The nematode *Caenorhabditis elegans* has been successfully used as a model species in many fields of biological research [6,7]. Because of a lack of an adaptive immune system, this tiny worm relies solely on its innate immune defense to cope with pathogen attacks. Therefore, the worm is widely used in the study of host innate immunity, and antibacterial molecules related to its innate immunity have been identified [8,9].

Antibacterial factor (ABF) is an antimicrobial peptide identified in *C. elegans* [10]. ABF was first found by a computer-assisted search of a database using the amino acid sequence of *Ascaris suum* antibacterial factor (ASABF) [11]. Both ABF and ASABF are thought to belong to a cysteine-stabilized α-helix and β-sheet (CSαβ) superfamily, which contains a single α-helix and a pair of anti-parallel β-sheets stabilized by three or four disulfide bridges. Until now, six kinds of ABF (ABF-1~6) have been identified from *C. elegans* [12]. Among these ABFs, the antimicrobial activity of only ABF-2 has been characterized. A previous study reported that ABF-2 has a broad antimicrobial spectrum compared to that of other CSαβ-type antimicrobial peptides. It has been reported that the C-terminal region of ABFs is longer and more widely diverse than that of other CSαβ-type antimicrobial peptides. Moreover, ABFs differ from the `classical' CSαβ-type antimicrobial peptides, such as drosomycin and plant defensins, in the spacing of half-cystine residues, cysteine pairings, and the organization of the precursor. Therefore, it is thought that the structural properties of ABFs may contribute to their broad antimicrobial spectrum. Although the CSαβ structure of

ASABF was solved by ^{1}H-NMR (Aizawa et al., manuscript in preparation), the structure of ABF-2 remains unclear. Therefore, the structural analysis of ABF-2 will provide new clues to clarify the structure-activity relationships of ABFs.

In general, recombinant production of antimicrobial peptides has been difficult because of their activity, although that is a useful technique for various studies. In addition, ABF-2 contains four intramolecular disulfide bridges, thus it is difficult to produce correctly folded and active ABF-2. There are two major methods for producing recombinant peptides that require the formation of disulfide bridges for proper folding and function. One method uses the yeast secretory expression system. Recombinant peptide expression in yeast has many advantages, such as disulfide bridge formation and proper folding [13]. The yeasts *Pichia pastoris* and *Saccharomyces cerevisiae* are widely used as expression hosts for recombinant peptides. However, a previous study reported that the expression level of ABF-2 in *P. pastoris* was extremely low (100 μg/L) [10]. In addition, in the case of overexpression of ASABF by using *P. pastoris*, it was reported that unfavorable degradation occurred in its C-terminus [11]. The other method is to refold the inclusion body into peptides with native conformations [14]. In this study, I chose *E. coli* as an expression host and tried to express ABF-2 as inclusion bodies in *E. coli*. Unfortunately, when it was overexpressed directly, ABF-2 was expressed at low yield as inclusion bodies in *E. coli*. In this study, therefore, I applied a coexpression method for the production of ABF-2 to enhance inclusion body formation. In this method, it is expected that coexpression of the aggregation-prone protein (partner protein) enhances the inclusion body formation of the peptide of interest (target peptide) and protects the target peptide from proteolytic degradation by protease. Moreover, I evaluated the effect of the charge of partner proteins on inclusion body formation of ABF-2 in this method by using four structurally homologous proteins. As far as I know, this is the first report to show experimentally that the isoelectric point of the coexpressed partner protein is an important factor for inclusion body formation of the target peptide.

1-3 Materials and Methods

Materials

E. coli DH5α was used as a host strain for cloning and for preparing template plasmids. *E. coli* BL21 (DE3) was used as an expression host. ^{15}N-labeled CHL medium was purchased from Chlorella Industry.

Construction of coexpression vector of ABF-2 and partner protein

The ABF-2 gene fragment was amplified by PCR with a set of primers (Table 1). This product was ligated to the pCOLADuet1 vector (Novagen) by using *Nde*I-*Xho*I sites (Fig. 1). This vector was designated pCOLA-ABF-2. In this study, I selected four kinds of aggregation-prone proteins (human α-lactalbumin (HLA), bovine α-lactalbumin (BLA), human lysozyme (HLZ), and bovine lysozyme (BLZ)) as partner proteins. The PCR-amplified partner protein gene fragments (HLA, BLA, HLZ, and BLZ) were digested using restriction enzymes, and each was subcloned into the pCOLA-ABF-2 vector by using *Nco*I-*Bam*HI sites. For instance, in this study, the pCOLA-ABF-2 vector containing the HLA gene was named pCOLA-[HLA]-ABF-2. The clone sequence was confirmed by capillary sequencing.

Evaluation of the partner protein's effect on ABF-2 expression level

E. coli BL21 (DE3) cells were transformed with the various expression constructs (pCOLA-[HLA]-ABF-2, pCOLA-[BLA]-ABF-2, pCOLA-[HLZ]-ABF-2, pCOLA-[BLZ]-ABF-2, and pCOLA-ABF-2). The transformed cells were grown at 37 ˚C in 5 mL of LB medium until the OD_{600} reached 1.0-1.2. The cells were induced by the addition of 1 mM IPTG and further cultivated for 4 h. The cells were harvested by centrifugation at 15,000 rpm for 5 min at 4 ˚C. After the cells were lysed using Bugbuster (Novagen),

inclusion bodies were isolated by centrifugation at 15,000 rpm for 5 min at 4 ℃ and analyzed on Tricine-SDS PAGE. The intensity of ABF-2 bands was quantified by densitometry.

Expression and purification of ABF-2

The *E. coli* strain BL21(DE3) harboring the pCOLA-[BLA]-ABF-2 vector was cultured overnight at 37 ℃ in 50 mL of LB medium containing 20 μg/mL kanamycin. This preculture was inoculated to 1 L of medium (LB or ^{15}N-CHL) containing 20 μg/mL kanamycin. The culture was grown at 37 ℃, and protein expression was induced by the addition of 1 mM IPTG when the OD_{600} reached 1.0-1.2. At this point, for the production of ^{15}N-labeled ABF-2, a ^{15}N-labeled algal amino acid mixture was added to the CHL medium according to the protocol provided by the supplier. After an additional 4 h cultivation, cells were harvested by centrifugation at 6,000 rpm for 10 min. The cells were resuspended in lysis buffer (20 mM Tris-HCl, 1 mM EDTA, pH 8.0) and disrupted by sonication. Next, inclusion bodies composed mainly of BLA and ABF-2 were isolated by centrifugation at 7,500 rpm for 30 min at 4 ℃. The inclusion bodies were washed twice with lysis buffer containing 0.1% TritonX-100 and washed once with lysis buffer (without TritonX-100).

The washed inclusion bodies were solubilized in solubilization buffer (8 M urea, 200 mM β-mercaptoethanol, 20 mM Tris-HCl, 3 mM EDTA, pH 8.0). After centrifugation at 7,500 rpm at 4 ℃ for 30 min, the clarified supernatant was loaded onto a HiTrap SP HP cation-exchange column (GE Healthcare) pre-equilibrated with equilibration buffer (8 M urea, 20 mM Tris-HCl, 20 mM β-mercaptoethanol, 3 mM EDTA, pH 8.0). The bound ABF-2 was eluted with a linear gradient of equilibration buffer with 0-600 mM NaCl. The fractions containing ABF-2 were identified using Tricine-SDS PAGE. These fractions were collected and dialyzed three times against refolding buffer (20 mM Tris-HCl, 2 mM reduced glutathione, 0.2 mM oxidized glutathione, pH 8.0) for 12 h at 4 ℃. Correctly folded ABF-2

was purified by RP-HPLC on a Cosmosil 5C18-AR-300 column (Nacalai Tesque). The elution was carried out with a linear gradient of 25-45% acetonitrile with 0.1% trifluoracetic acid. The yield of ABF-2 was determined by measuring the absorbance at 280 nm. The purified recombinant ABF-2 was lyophilized and stored at -30 ℃.

Microbicidal assay

The antimicrobial activity of ABF-2 against *S. aureus* ATCC6538P and *E. coli* K12 was tested by a colony-forming unit assay. Bacteria were grown in tryptic soy broth (TSB) and collected in the mid-log phase by centrifugation. The bacteria were washed and diluted in sterile water. Various concentrations of ABF-2 were incubated with 1×10^7 bacteria in a final volume of 50 μL at 37 ℃ for 2 h. After incubation, 1,000-fold dilutions were prepared and 100 μL of the diluted samples was plated on a solid medium comprised of TSB. The plates were incubated for 20 h at 37 ℃ and then the colonies were counted. The results indicated a 50% bactericidal concentration (BC_{50}).

Circular dichroism spectroscopy analysis

Circular dichroism (CD) spectra were measured in 1 mm path length quartz cuvettes on a J-725 spectropolarimeter (Jasco) equipped with a temperature control device. Spectra were acquired over a wavelength range between 250 nm and 200 nm as an average of four spectra with a 50 nm/min scan speed and a step resolution of 0.1 nm at 25 ℃. ABF-2 samples (50 μM) were used in buffer (20 mM Tris-HCl, pH 8.0). Blank was subtracted from all spectra. All measurements were averaged and converted to molar ellipticity.

NMR spectroscopy

^{15}N-labeled ABF-2 was dissolved in 20 mM phosphate buffer (pH 5.7) comprising a 90% H_2O/10% D_2O mixture. NMR experiments were performed on a JEOL ECA-600 and a

Bruker AVANCE III 800 spectrometer with a TCI cryogenic probe. The ^{1}H-^{15}N heteronuclear single quantum coherence (HSQC) spectrum was collected at 20 ℃. The data were processed by using NMRpipe/NMRdraw [15].

1-4 Results

Construction and expression of coexpression plasmids encoding ABF-2 and partner proteins

First, I tried to express ABF-2 as an inclusion body in *E. coli*, but the expression level of ABF-2 was extremely low (Fig. 2). To enhance the inclusion body formation of ABF-2, I decided to apply a coexpression method.

To construct a coexpression plasmid containing ABF-2 and aggregation-prone partner protein genes, I utilized the commercially available pCOLADuet1 vector from Novagen. This vector has two RBS sites flanking two multiple cloning sites, and these are under the control of each T7 promoter. In this study, partner protein genes were subcloned into the first multiple cloning site of the pCOLA vector, and the ABF-2 gene was subcloned into the second multiple cloning site of the pCOLA vector.

To evaluate the effect of a partner protein on the ABF-2 expression level, various partner proteins and ABF-2 were coexpressed (Table 2). The expression of ABF-2 was moderately increased in the case of the coexpression of ABF-2 and BLZ (Fig. 2). The expression of ABF-2 was markedly increased as an inclusion body by coexpression of HLA or BLA. On the other hand, the expression level of ABF-2 was not affected, although HLZ was clearly overexpressed as an inclusion body. Because the expression level of ABF-2 was increased the most by coexpression of BLA, I selected BLA as a partner protein for large-scale production of ABF-2.

Purification and refolding of ABF-2

ABF-2 was easily separated from BLA by using cation-exchange chromatography under denaturing conditions, because of the opposite charge (Fig. 3). Unlike fusion protein systems, there was no need to remove the fusion protein tag by enzymatic or

chemical methods. After cation-exchange chromatography, I obtained about 54 mg of crude ABF-2 without disulfide bonds from 1 L of *E. coli* culture. Next, this crude ABF-2 was refolded by dialysis. After the refolding and purification procedure, I obtained 7.8 mg of correctly folded ABF-2 from 1 L culture.

Antimicrobial activity of recombinant ABF-2

The microbicidal activity of recombinant ABF-2 was examined (Table 3). The 50% microbicidal concentrations were 0.01 and 0.1 μM for *S. aureus* and *E. coli*, respectively. The Gram-positive bacterium (*S. aureus*) is 10-fold more sensitive than the Gram-negative bacterium (*E. coli*). Neither *S. aureus* nor *E. coli* was sensitive to the misfolded fraction (data not shown).

Circular dichroism spectrum of ABF-2

Furthermore, to confirm that purified ABF-2 was folded correctly, the CD spectra of ABF-2 were measured. The spectra of misfolded ABF-2 revealed a random coil structure (Fig. 4). On the other hand, the CD spectra of refolded ABF-2 showed significant decreases in molar ellipticity values in the region between 208 and 220 nm. This indicates that a secondary structure was formed in refolded ABF-2.

^{1}H-^{15}N HSQC spectrum of ^{15}N-labeled ABF-2

The large amount of isotopically labeled ABF-2 enabled the rapid and sensitive acquisition of NMR spectra. The HSQC spectrum of ^{15}N-labeled ABF-2 is presented in Fig. 5. The number of peaks in the HSQC spectrum of ^{15}N-labeled ABF-2 corresponded approximately to the number of residues in ABF-2. The majority of the ^{1}H-^{15}N cross-peaks lay between 7.5 and 9.5 ppm. The sharp, well-dispersed peaks indicate that purified ABF-2 was correctly folded.

1-5 Discussion

Because the correct disulfide arrangements of disulfide-containing peptides are difficult to obtain, the yeast *P. pastris* is widely used to express peptides containing intramolecular disulfide bridges. The main advantage of *P. pastris* as a host is that it is expected to secrete peptides with correct disulfide bridges directly into culture medium [16]. Several CSαβ-type antimicrobial peptides were produced by using *P. pastris*, and these were well characterized [17-19]. However, a previous study showed that *P. pastris* is not a suitable host for large-scale production of ABF-2. Although the antimicrobial spectrum of ABF-2 was investigated, structural and mutational studies of ABF-2 have not yet been conducted because of the low yield of ABF-2 in *P. pastris* [10]. Therefore, it is very important to develop an alternative expression method that enhances the expression level of ABF-2.

In this study, I selected *E. coli* as an expression host and at first tried to express ABF-2 directly in *E. coli* as inclusion body. Unfortunately, the direct expression of ABF-2 in *E. coli* was insufficient due to the instability of the expressed ABF-2 itself in the cells (Fig. 2). I speculated that this low-level expression of ABF-2 was caused by the degradation of expressed ABF-2 by proteases of *E. coli*. Therefore, I thought that the prevention of ABF-2 degradation by proteases is essential to enhance the expression level of ABF-2 as inclusion bodies.

To prevent the degradation of target peptides, fusion protein systems have generally been used in many studies. The attachment of soluble proteins to target peptides has been observed to prevent degradation and promote proper folding [20]. However, when an antimicrobial peptide like ABF-2 is expressed in a soluble form, it may damage host cells by disrupting their cell membranes. Moreover, in fusion protein systems, enzymatic or chemical cleavage is inevitable to remove the fusion protein tag.

Enzymatic cleavage often degrades recombinant peptides, because widely used proteases, such as enterokinase and factor Xa, often show nonspecific cleavages at unexpected sites. Furthermore, many peptides often contain potential cleavage sites cleaved by chemicals. For instance, CNBr is commonly used to cleave peptide bonds C-terminal to methionine residues in proteins and peptides. However, because ABF-2 contains methionine in its amino acid sequence, CNBr cannot be used to separate ABF-2 from the fusion protein.

Expression of inclusion bodies may also be useful to avoid proteolytic degradation of the target peptide. However, it is difficult to control inclusion body formation in *E. coli* cells. As another way to produce fusion proteins, the utilization of insoluble protein tags was also reported [21]. In that case, both degradation and toxicity are expected to be prevented. However, when an insoluble protein tag is used for fusion expression, it is difficult to use enzymatic cleavage because of the insolubility of the fusion protein, and chemical cleavage is usually the only way to induce cleavage. Thus, this cleavage step is one of the obstacles of this method.

In some reports the coexpression of an insoluble partner protein enhances the inclusion body formation of the target peptide and protects it from proteolytic degradation by protease. Saito *et al*. reported that the expression level of somatomedin C is enhanced in the case of coexpression of insulin-like growth factor I [22]. Jang *et al*. succeeded in producing a potent antimicrobial peptide, buforin IIb, by coexpression of human gamma interferon [23]. To obtain a large amount of ABF-2, I decided to apply this method to ABF-2 and examine the effects of aggregation-prone partner proteins in detail.

In previous studies, translationally coupled two-cistron plasmids were used to coexpress target peptides and partner proteins [22, 23]. However, genetic manipulation was needed to construct translationally coupled two-cistron expression systems. In the present study, I simply used the commercially available pCOLADuet-1 vector to

coexpress ABF-2 and partner protein genes (Fig. 1). Because this vector is designed for the cloning and coexpression of two genes, the construction of a coexpression plasmid is very easy. Therefore, my method can be easily applied to many proteins and peptides.

In this study, I chose four kinds of proteins as aggregation-prone partners. Lysozyme and α-lactalbumin appear to have evolved from a common ancestral protein, as evidenced by the similarity of their amino acid sequences and three-dimensional structures as well as by the high conservation of disulfide bridges [24]. Some studies clearly showed that these four proteins each form a large amount of inclusion bodies when overexpressed in *E. coli* [25, 26]. Interestingly, the isoelectric points of these proteins are different despite their sequential similarity. Thus, I selected these proteins as good models of aggregation-prone partners in order to evaluate the effect of the charge of the partner protein on the expression level of cationic ABF-2 (pI 9.1).

Coexpression of BLZ, whose isoelectric point is 6.5, modestly enhanced the expression level of ABF-2. In contrast, ABF-2 was produced effectively as an inclusion body in the case of coexpression with an anionic partner protein (HLA or BLA). On the other hand, the expression level of ABF-2 was not changed by coexpression of HLZ, whose isoelectric point is high. Although it has been thought that the charge of both target and partner proteins influences inclusion body formation, the effect of the charge of the partner protein on the expression level of the target peptide has not been elucidated in detail. In this study, I experimentally showed that the charge of the partner protein is an important factor for enhancing the inclusion body formation of the target peptide. Interestingly, although HLA and BLA have almost the same isoelectric points and molecular weights, the expression level of ABF-2 was enhanced more by coexpression of BLA than by that of HLA. Because not only electrostatic but also hydrophobic interactions are thought to be critical factors for inclusion body formation [27], I compared their GRAVY scores, which express the total hydrophobicity of a

protein. However, I could not find a correlation between the expression level of ABF-2 and the GRAVY scores of the partner proteins. There may be unknown factors that affect inclusion body formation.

It has been reported that the presence of impurities in an inclusion body, such as nucleic acids and non-plasmid-encoded proteins, affects the final refolding yield of the target [28]. These impurities can be removed by washing the body using a low concentration of detergent. Therefore, inclusion body washing is very important to enhance the refolding yield of the target. However, in this study I observed that the inclusion body composed of ABF-2 without partner proteins was gradually solubilized during the washing process (data not shown). Because of this unfavorable solubilization of the body, ABF-2 was lost during the washing process and I could not obtain even crude ABF-2 in the case of expression without partner proteins. On the other hand, the inclusion body composed of ABF-2 and the partner protein was hardly solubilized during the washing process. It seems that the robust inclusion body is formed in the case of coexpression with the partner protein. From these results, it can be said that coexpression of an aggregation-prone protein is effective not only in enhancing the expression level of a target peptide as an inclusion body but also in preventing the unfavorable loss of an inclusion body during washing.

Because ABF-2 has a charge that is opposite that of BLA, I succeeded in separating ABF-2 from BLA efficiently by a simple one-step cation-exchange chromatography without enzymatic or chemical cleavage (Fig. 3). After cation-exchange chromatography, I succeeded in obtaining 54 mg of crude ABF-2 without disulfide bridges from 1 L of culture. Although crude ABF-2 was refolded by a very simple standard dialysis refolding protocol, I obtained as much as 7.8 mg of correctly folded ABF-2. Because refolding additives, such as arginine, have been used to suppress the aggregation of proteins during refolding in many studies [29], optimization of the

refolding protocol may enhance the refolding yield of ABF-2.

To confirm that refolded ABF-2 was correctly folded and active, purified ABF-2 was evaluated by colony-forming unit assay as well as by CD and NMR spectroscopy (Table 3, Figs. 4, 5). I confirmed that purified ABF-2 was active against both *S. aureus* and *E. coli*. Moreover, *S. aureus* is more sensitive than *E. coli*. These results were identical to previous results [10]. Quantitative analysis of the CD spectra of purified ABF-2 indicated a secondary structural content of 28% α-helix, 17% β-sheet. This result was in agreement with the categorization of ABF-2 as a CSαβ-type antimicrobial peptide. Moreover, the HSQC spectrum of ^{15}N-labeled ABF-2 is sharp and well dispersed. From these data, I concluded that purified ABF-2 was correctly folded. This sample will enable me to analyze the structure and interaction of ABF-2 by using NMR in future studies.

It is known that the long C-terminal regions of ABFs are divergent and vary in length [12]. Therefore, the difference in the C-terminal region of ABFs is thought to affect their antimicrobial spectrum. I think that my method described in this work can be applied not only to ABF-2 but also to other ABFs. By using this method, I are going to elucidate the effects of the differences in the C-terminal regions of ABFs on their antimicrobial spectra.

1-6 References

[1] T. Gnaz, The role of antimicrobial peptides in innate immunity, Integr. Comp. Biol. 43 (2003) 300-304.

[2] K. Radek, R. Gallo, Antimicrobial peptides: natural effectors of the innate immune system, Semin. Immunol. 29 (2007) 27-43.

[3] H. Sato, J.B. Feix, Peptide-membrane interactions and mechanisms of membrane destruction by amphipathic α-helical antimicrobial peptides, Biochim. Biophys. Acta. 1758 (2006) 1245-1256.

[4] R. Mani, A.J. Waring, R.I. Lehrer, M. Hong, Membrane-disruptive abilities of beta-hairpin antimicrobial peptides correlate with conformation and activity: a 31P and 1H NMR study, Biochim. Biophys. Acta. 1716 (2005) 11-18.

[5] M. Zasloff, Antimicrobial peptides of multicellular organisms, Nature 415 (2002) 389-395.

[6] T. Kaletta, M.O. Hengartner, Finding function in novel targets: *C. elegans* as a model organism, Nat. Rev. Drug Discov. 5 (2006) 387-398.

[7] A.J. Walhout, R. Sordella, X. Lu, J.L. Hartley, G.F. Temple, M.A. Brasch, N. Thierry-Mieg, M. Vidal, Protein interaction mapping in *C. elegans* using proteins involved in vulval development, Science 287 (2000) 116-122.

[8] H. Schulenburg, C.L. Kurz, J.J. Ewbank, Evolution of the innate immune response: the worm perspective, Immunol. Rev. 198 (2004) 36-58.

[9] T. Roeder, M. Stanisak, C. Gelhaus, I. Bruchhaus, J. Grotzinger, M. Leippe, Caenopores are antimicrobial peptides in the nematode *Caenorhabditis elegans* instrumental in nutrition and immunity, Dev. Comp. Immunol. 34 (2010) 203-209.

[10] Y. Kato, T. Aizawa, H. Hoshino, K. Kawano, K. Nitta, H. Zhang, *abf*-1 and *abf*-2, ASABF-type antimicrobial peptide genes in *Caenorhabditis elegans*, Biochem. J. 361 (2002) 221-230.

[11] H. Zhang, S. Yoshida, T. Aizawa, R. Murakami, M, Suzuki, N. Koganezawa, A. Matsuura, M. Miyazawa, K. Kawano, K. Nitta, Y. Kato, In vitro antimicrobial properties of recombinant ASABF, an antimicrobial peptide isolated from the nematode *Ascaris suum*, Antimicrob. Agents Chemother. 44 (2000) 2701-2705.

[12] O. Froy, Convergent evolution of invertebrate defensins and nematode antibacterial factors, Trends Microbiol. 13 (2005) 314-319.

[13] D. Porro, M. Sauer, P. Branduardi, D. Mattanovich, Recombinant protein production in yeasts, Mol. Biotechnol. 31 (2005) 245-259.

[14] S.M. Singh, A.K. Panda, Solubilization and refolding of bacterial inclusion body proteins, J. Biosci. Bioeng. 99 (2005) 303-310.

[15] F. Delaglio, S. Grzesiek, GW. Vuister, G. Zhu, J. Pfeifer, A. Bax, NMRPipe: a multidimensional spectral processing system based on UNIX pipes, J. Biomol. NMR. 6 (1995) 277-293.

[16] R. Daly, M.T. Hearn, Expression of heterologous proteins in *Pichia pastoris*: a useful experimental tool in protein engineering and production, J. Mol. Recognit. 18 (2005) 119-138.

[17] L. Wang, C. Lai, Q. Wu, J. Liu, M. Zhou, Z. Ren, D. Sun, S. Chen, A. Xu, Production and characterization of a novel antimicrobial peptide HKABF by *Pichia pastoris*, Process Biochem. 43 (2008) 1124-1131.

[18] J. Zhang, Y.L. Yang, D. Teng, Z.G. Tian, S.R. Wang, J.H. Wang, Expression of plectasin in *Pichia pastoris* and its characterization as a new antimicrobial peptide against *Staphyloccocus* and *Streptococcus*, Protein. Expr. Purif. 78 (2011) 189-196.

[19] M. Wiens, H.C. Schröder, M. Korzhev, X-H. Wang, R. Batel, WEG. Müller, Inducible ASABF-type antimicrobial peptide from the sponge *Suberites domuncula*: Microbicidal and hemolytic activity *in vitro* and toxic effect on molluscs *in vivo*, Mar. Drugs. 9 (2011) 1969-1994.

[20] Z. Xu, L. Peng, Z. Zhong, X. Fang, P. Cen, High-level expression of a soluble functional antimicrobial peptide, human βdefensin 2, in *Eschcherichia coli*, Biotechnol. Prog. 22 (2006) 382-386.

[21] T.J. Park, J.S. Kim, S.S. Choi, Y. Kim, Cloning, expression, isotope labeling, purification, and characterization of bovine antimicrobial peptide, lactophoricin in *Escherichia coli*, Protein. Expr. Purif. 65 (2009) 23-29.

[22] Y. Saito, Y. Ishii, M. Niwa, I. Ueda, Direct expression of a synthetic somatomedin C gene in *Escherichia coli* by use of a two-cistron system, Journal of Biochemistry 101 (1987) 1281-1288.

[23] S.A. Jang, B.H. Sung, J.H. Cho, S.C. Kim, Direct expression of antimicrobial peptides in an intact form by a translationally coupled two-cistron expression system, Appl. Environ. Microbiol. 75 (2009) 3980-3986.

[24] H.A. McKenzie, F.H. White. Lysozyme and α-lactalbumin: structure, function, and interrelationships, Adv Protein. Chem. 41 (1991) 173-315.

[25] M. Svensson, A. Håkansson, AK. Mossberg, S. Linse, C. Svanborg, Conversion of α-lactalbumin to a protein inducing apoptosis, Proc. Natl. Acad. Sci. U. S. A. 97 (2000) 4221-4226.

[26] M. Li, Z. Su. Refolding human lysozyme produced as an inclusion body by urea concentration and pH gradient ion exchange chromatography, Chromatographia. 56 (2002) 33-38.

[27] M. Murby, E. Samuelsson, T.N. Nguyen, L. Mignard, U. Power, H. Binz, M. Uhlen, Ståhl S. Hydrophobicity engineering to increase solubility and stability of a recombinant protein from respiratory syncytial virus, Eur. J. Biochem. 230 (1995) 38-44.

[28] J. Maachupalli-Reddy, B.D. Kelley, E.D.B. Clark, Effect of inclusion body contaminants on the oxidative renaturation of hen egg white lysozyme, Biotechnol. Prog. 13

(1997) 144-150.

[29] T. Arakawa, D. Ejima, K. Tsumoto, N. Obeyama, Y. Tanaka, Y. Kita, S.N. Timasheff, Suppression of protein interactions by arginine: a proposed mechanism of the arginine effects, Biophys. Chem. 127 (2007) 1-8.

Table 1 Sequences of primers used in this study

Name	Primer sequence[a] (from 5' end to 3' end)	Restriction site
Primers for ABF-2 gene	F = GGAATTCCATATGGACATCG ACTTTAGTACTTGTGC	*Nde*I
	R = CCGCTCGAGTTATCCTCTCT TAATAAGAGCACCAAG	*Xho*I
Primers for HLA gene	F = GAATTCTCATGAAGCAATTC ACAAAATGTGAGCTG	*Bsp*HI
	R = CGGGATCCTTACAACTTCTC ACAAAGCCACTG	*Bam*HI
Primers for BLA gene	F = GAATTCCCATGGAACAGTTA ACAAAATGTGAGGTG	*Nco*I
	R = CGGGATCCTTACAACTTCTC ACAGAGCCA	*Bam*HI
Primers for HLZ gene	F = GAATTCTCATGAAGGTCTTT GAAAGGTGTGAGTTG	*Bsp*HI
	R = CGGGATCCTTACACTCCACA ACCTTGAACATAC	*Bam*HI
Primers for BLZ gene	F = GAATTCTCATGAAGGTCTTT GAGAGATGTGAGC	*Bsp*HI
	R = CGGGATCCTTACAGGGTGCA ACCCTCAA	*Bam*HI

a. Restriction sites are underlined.

Table 2 Properties of antibacterial factors and partner proteins used in this study.

Name	Mw	pI	GRAVY score[a]
antibacterial factor 2 (ABF-2)	6999.2	9.1	-0.072
human α-lactalbumin (HLA)	14078.2	4.7	-0.255
bovine α-lactalbumin (BLA)	14186.1	4.8	-0.453
human lysozyme (HLZ)	14700.7	9.3	-0.485
bovine lysozyme (BLZ)	14415.2	6.5	-0.395

a. GRAVY stands for grand average of hydropathy. The Positive GRAVY scores indicate hydrophobic peptides, and negative scores indicate hydrophilic peptides.

Table 3 Microbicidal activity of recombinant ABF-2

Organism	BC_{50} (μM)
Gram-positive bacteria	
Staphylococcus aureus (ATCC6538P)	0.01
Gram-negative bacteria	
E. coli (K12)	0.1

Microbicidal activity was assessed as 50% microbicidal concentration (BC_{50}).

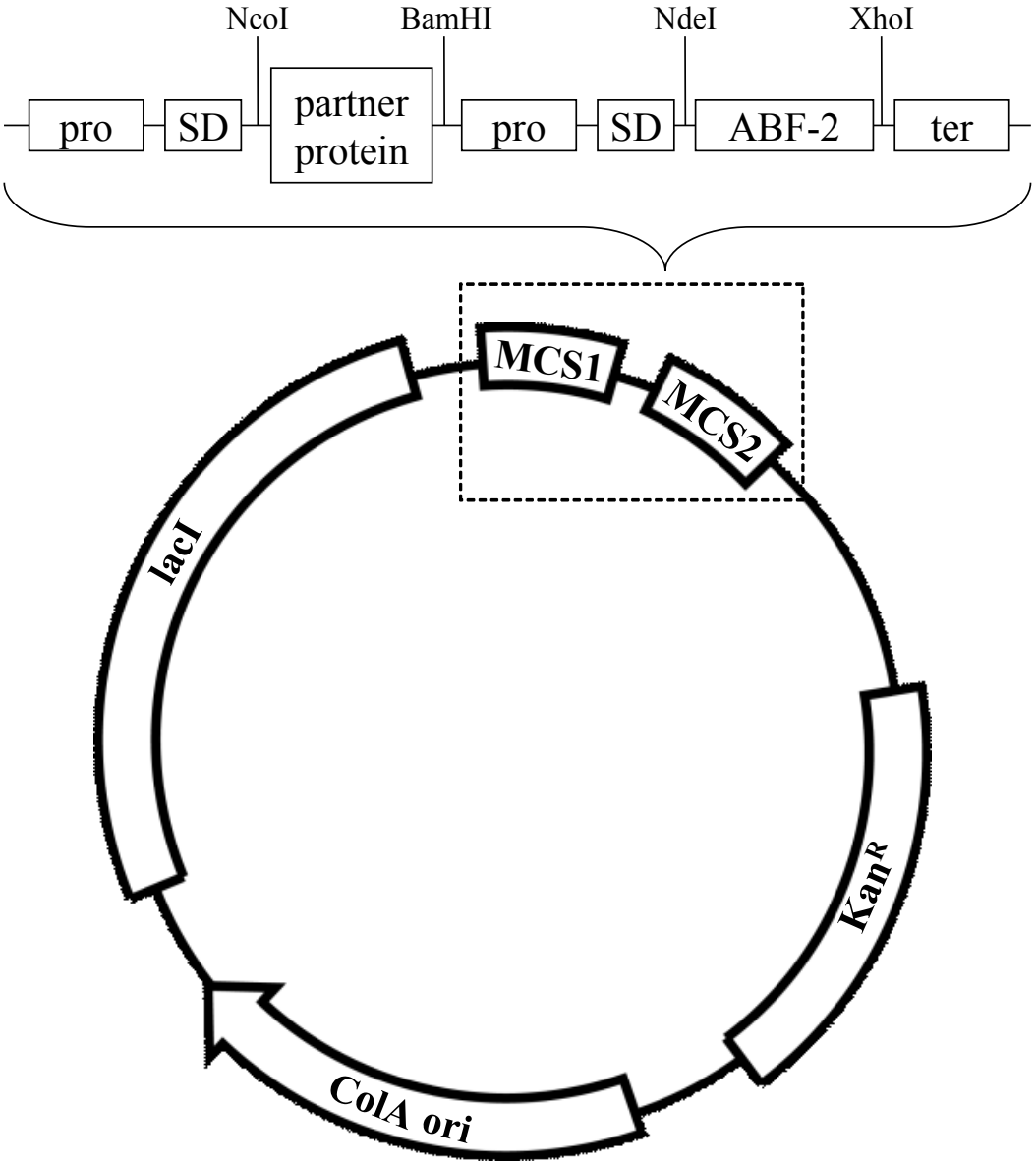

Figure 1. Schematic representation of expression vector. pro, T7 promoter; SD, Shine-Dalgarno sequence; ter, T7 terminator.

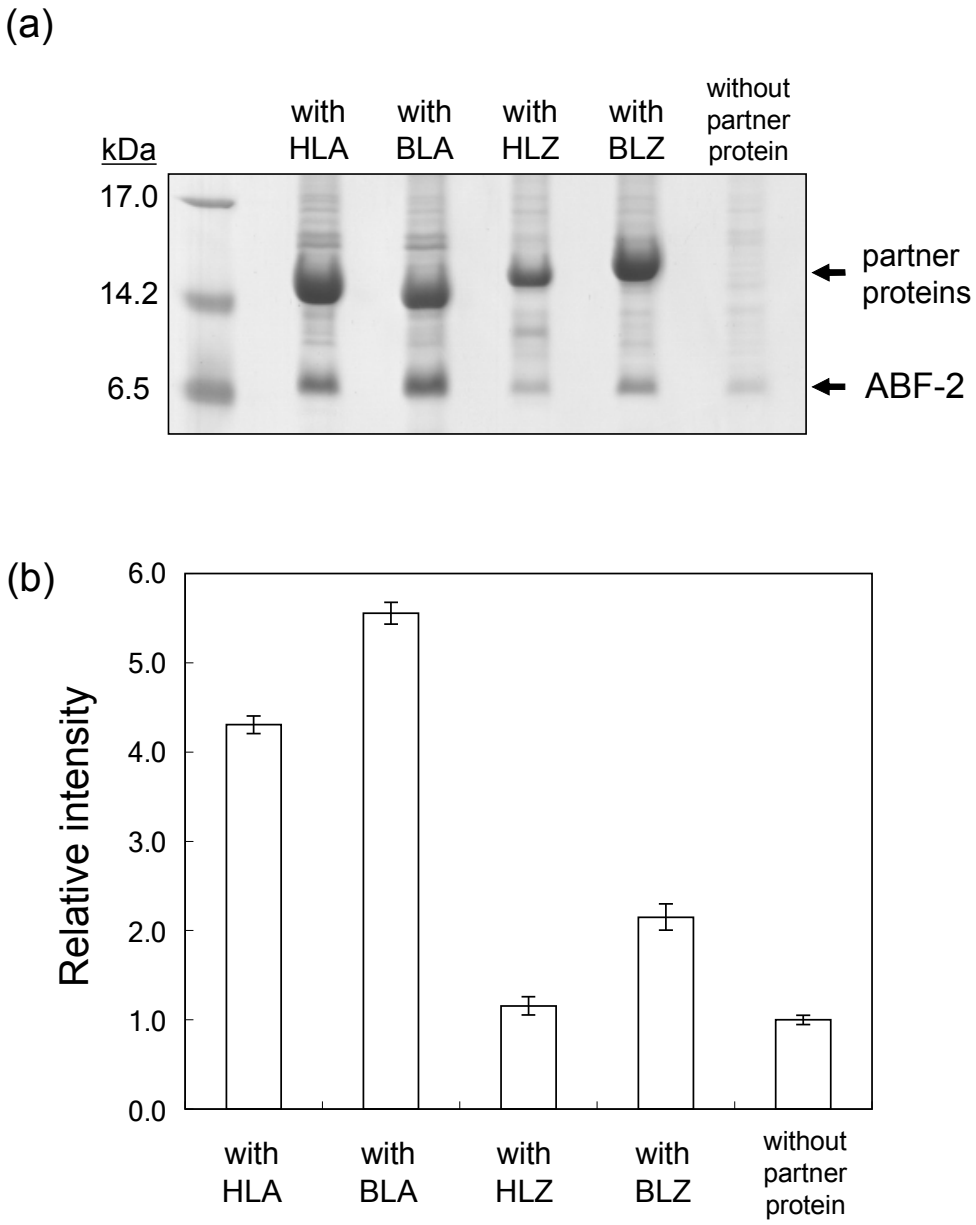

Figure 2. Effects of the charges of the partner proteins on ABF-2 expression level. (a): Tricine-SDS-PAGE analysis of the expression level of ABF-2. (b): The intensity data of the coexpression method are expressed in relation to those for the direct expression method. The graph represents the average intensities of three independent experiments.

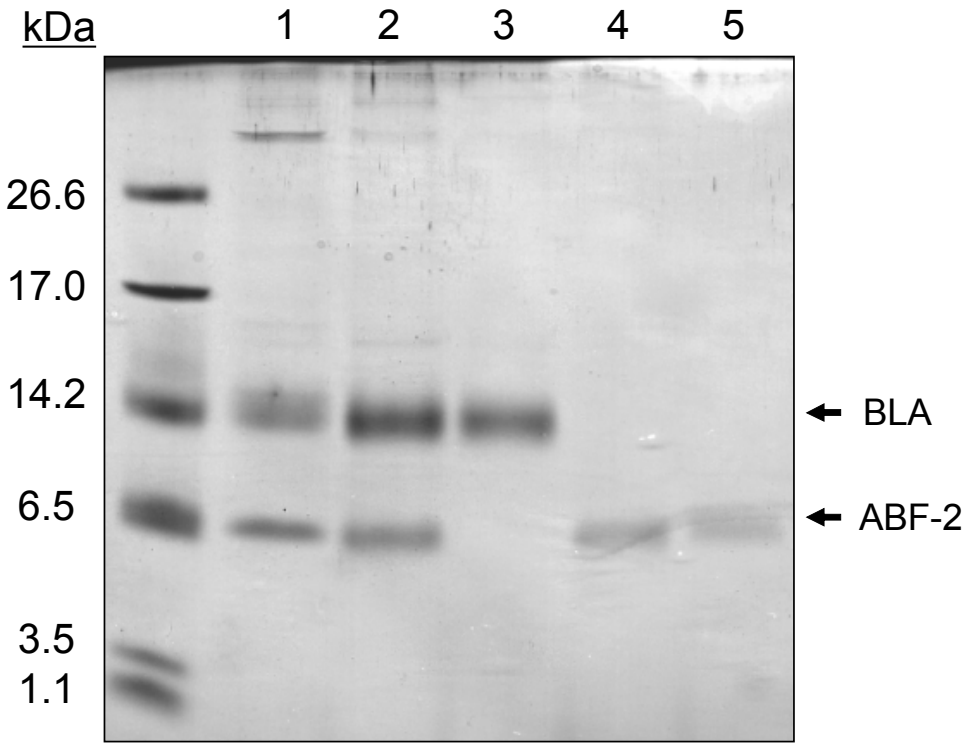

Figure 3. Expression and purification of recombinant ABF-2. Lane 1: Inclusion body after ultrasonication and centrifugation. Lane 2: Solubilized inclusion body. Lane 3: Flowthrough fraction that passed through cation-exchange chromatography. Lane 4: Purified ABF-2 using cation-exchange chromatography. Lane 5: Purified correctly folded ABF-2 using RP-HPLC.

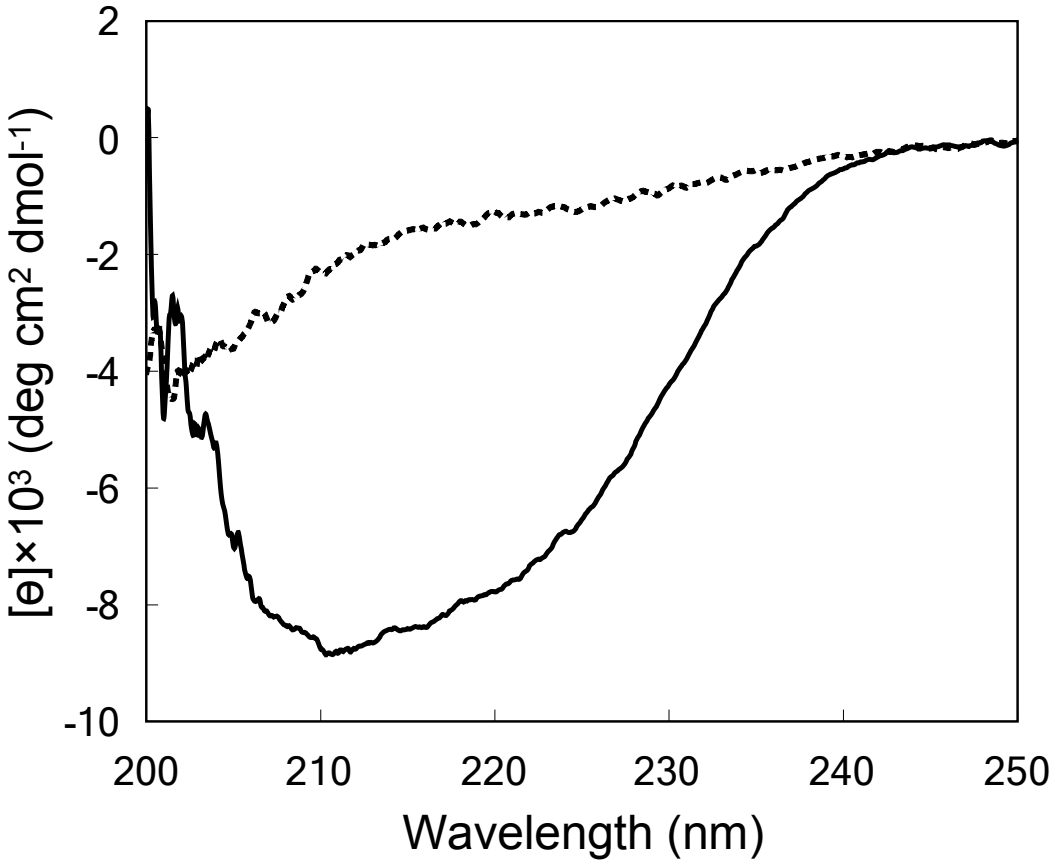

Figure 4. Circular dichroism spectra of correctly folded (solid line) and misfolded (dotted line) ABF-2.

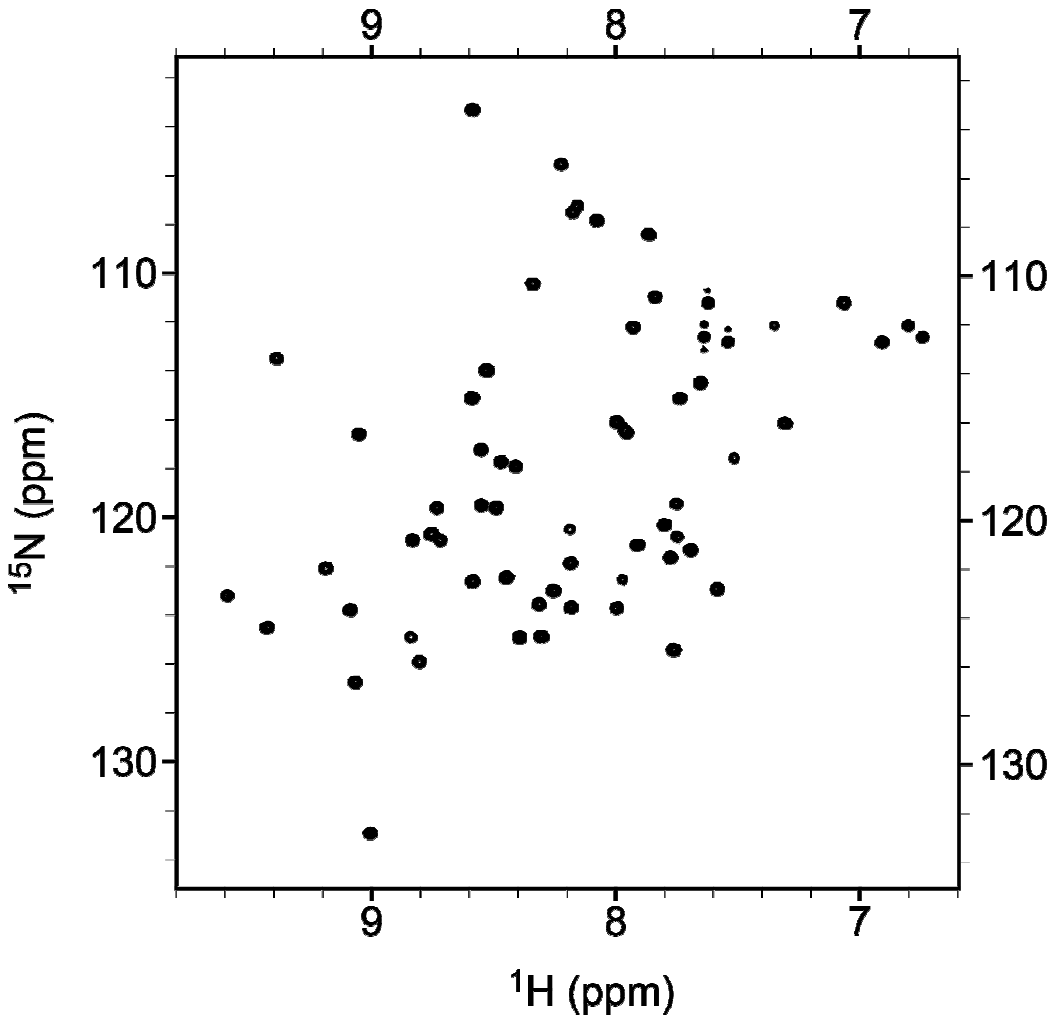

Figure 5. ^{1}H-^{15}N HSQC spectrum of 0.7 mM ^{15}N-labeled ABF-2 in 20 mM phosphate buffer at pH 5.7 and 20 ℃.

Chapter 2

Efficient production of a correctly folded mouse α-defensin, cryptdin-4, by refolding during inclusion body solubilization

2-1 Abstract

Mammalian α-defensins contribute to innate immunity by exerting antimicrobial activity against various pathogens. To perform structural and functional analysis of α-defensins, large amounts of α-defensins are essential. Although many expression systems for the production of recombinant α-defensins have been developed, attempts to obtain large amounts of α-defensins have been only moderately successful. Therefore, in this study, I applied a previously developed coexpression method for the production of mouse α-defensin cryptdin-4 (Crp4) in order to enhance the formation of inclusion bodies by Crp4. By using this method, I succeeded in obtaining a large amount of Crp4 in the form of inclusion bodies. Moreover, I attempted to refold Crp4 directly during the inclusion-body solubilization step under oxidative conditions. Surprisingly, even without any purification, Crp4 was efficiently refolded during the solubilization step of inclusion bodies, and the yield was better than that of the conventional refolding method. NMR spectra of purified Crp4 suggested that it was folded into its correct tertiary structure. Therefore, the method described in this study not only enhances the expression of α-defensin as inclusion bodies, but also eliminates the cumbersome and time-consuming refolding step.

2-2 Introduction

Cationic antimicrobial peptides produced by animal cells represent the first line of defense against invasion by pathogens [1]. Defensins and cathelicidins are the two major classes of mammalian antimicrobial peptides [2]. Previous studies have shown that defensins are microbicidal against Gram-positive and Gram-negative bacteria, yeast, fungi, spirochetes, protozoa, and enveloped viruses [3,4]. Moreover, some defensins are known to act as chemokines that activate the adaptive immune response [2-5]. The mammalian defensins are characterized by six cysteine residues forming three intramolecular disulfide bridges, and are divided into two subfamilies, α- and β-defensins, based on the amino acid sequence similarities and the linkages of the disulfide bonds [3-5].

The α-defensins are cationic, amphipathic 3-4 kDa peptides [5]. They were first isolated from myeloid cells and later identified in intestinal Paneth cells. Structurally, α-defensins are characterized by a triple-stranded β-sheet structure that is constrained by three invariant disulfide bonds between Cys^{I}-Cys^{VI}, Cys^{II}-Cys^{IV}, and Cys^{III}-Cys^{V}. This characteristic pattern of disulfide bridges is considered to be crucial for maintenance of the three-dimensional structure and proteolytic stability of these peptides [5]. Moreover, α-defensins have conserved biochemical features including a canonical Arg-Glu salt bridge, a conserved Gly residue at Cys^{III+8}, and high content of Arg relative to that of Lys.

The mouse Paneth cell α-defensins, termed cryptdins (Crps), are secreted into the lumen of the small intestinal crypts in response to exposure to bacteria or bacterial antigens [6]. Among the known isoforms, cryptdin-4 (Crp4) has the most potent antimicrobial activity [7]. Furthermore, the primary structure of Crp4 uniquely lacks three amino acids residues between the fourth and fifth cysteine residues [7]. Because Crp4 has these features that distinguish it from other Crps, Crp4 has been studied most intensively. The solution structure of Crp4 has been determined by NMR spectroscopy [8,9]. Moreover, until now,

cysteine-deleted mutants [10,11], salt bridge-deficient mutants [9,12], positive-to-negative charge-reversal mutants [13] and an Arg-to-Lys mutant of Crp4 [14,15] have been studied to elucidate the role of the conserved biochemical features of α-defensins. In previous studies, the wild-type and mutants of Crp4 were prepared using the *Escherichia coli* expression system [8-15]. In this expression system, the recombinant wild-type and Crp4 mutants are expressed in *E. coli* as N-terminally linked, 6-histidine-tagged fusion peptides.

Large quantities of correctly folded α-defensin are essential to study the structure and antimicrobial activity of α-defensin. In general, it is difficult to obtain large amounts of α-defensins from natural sources due to their low concentration in these materials. Although chemically synthesized α-defensins were widely used in some previous studies [16-19], the chemical synthesis of α-defensin is very costly. Therefore, many strategies have been developed to produce α-defensin using recombinant techniques [20-25]. Because *E. coli* is easy to handle, is inexpensive, and grows quite fast, *E. coli* is the most widely used host strain for the overproduction of α-defensin [20-23]. However, the recombinant production of α-defensins using *E. coli* has been difficult due to their toxicity and proteolytic susceptibility.

To prevent their degradation, α-defensins are usually expressed as fusion proteins in *E. coli* cells [20-23]. The attachment of soluble protein to α-defensins has been adopted to prevent degradation and promote proper folding [22]. However, the soluble expression of antimicrobial peptides such as α-defensins may cause damage to the host cells by disrupting their cell membranes. Moreover, in fusion protein systems, enzymatic or chemical cleavage is necessary to remove fusion protein tags [20-23]. Enzymatic cleavage often causes unfavorable degradation of recombinant peptides, because widely used proteases, such as enterokinase and factor Xa, often show non-specific cleavages at unexpected sites [26,27]. Furthermore, many peptides often contain potential cleavage sites cleaved by chemicals. For instance, CNBr is commonly used to cleave peptide bonds C-terminal to methionine

residues in proteins and peptides [28]. However, because many α-defensins contain methionine in their amino acid sequences, CNBr cannot be used to separate such α-defensins from fusion proteins.

On the other hand, the formation of inclusion bodies may also be useful to avoid proteolytic degradation of α-defensins. However, it is difficult to control inclusion body formation in *E. coli* cells. As another way to produce fusion expression, utilization of insoluble protein tags has also been reported [20,23]. While this method prevents both degradation and toxicity, it does not readily allow the use of enzymatic cleavage due to the insolubility of the fusion protein, and thus chemical cleavage is the only practical method for cleavage. Moreover, when α-defensins are expressed in an insoluble form, they must be refolded in order to finally yield a correctly folded peptide. Thus, these cleavage and refolding steps are the drawbacks of this method.

Therefore, I here applied the coexpression method [29] to produce mouse α-defensin Crp4 in order to enhance the inclusion body formation. By using this method, it was expected that coexpression of the aggregation-prone protein (partner protein) would enhance inclusion body formation by the peptide of interest (target peptide) while simultaneously protecting the target peptide from proteolytic degradation by protease. Moreover, I attempted to refold Crp4 directly during the inclusion-body solubilization step under oxidative conditions. Interestingly, even without any purification, Crp4 was efficiently refolded in the solubilization step, and the yield was better than that by the conventional refolding method.

2-3 Materials and Methods

Bacterial strains

E. coli DH5α was used as a host strain for cloning and for preparing template plasmids. *E. coli* BL21 (DE3) was used as an expression host.

Construction of a vector coexpressing Crp4 and a partner protein

The Crp4 gene (GenBank accession no. NM010039) fragment was amplified by PCR with a set of primers using the cDNA-containing vector as template (Table 1). This product was ligated to the pCOLADuet1 vector (Novagen) by using NdeI-XhoI sites (Fig. 1), and the resulting vector was designated pCOLA-Crp4. In this study, I selected two aggregation-prone proteins, human α-lactalbumin (HLA; GenBank accession no. NM002289) and Cys-less human α-lactalbumin (Cys-less HLA), as partner proteins. The cDNA of Cys-less HLA was synthesized by Eurofins MWG Operon. In this mutant, all eight Cys residues in HLA were replaced by Ser. The PCR-amplified partner protein gene fragments (HLA and Cys-less HLA) were digested using restriction enzymes, and each was subcloned into the pCOLA-Crp4 vector by using NcoI-BamHI sites. For instance, in this study, the pCOLA-Crp4 vector containing the HLA gene was named pCOLA-[HLA]-Crp4. The clone sequence was confirmed by capillary sequencing.

Evaluating the effect of Cys residues of HLA on the Crp4 expression level

E. coli BL21 (DE3) cells were transformed with the various expression constructs (pCOLA-[HLA]-Crp4, pCOLA-[Cys-less HLA]-Crp4, and pCOLA-Crp4). The transformed cells were grown at 37°C in 5 mL of LB medium until the OD600 reached 1.0-1.2. The cells were induced by the addition of 1 mM IPTG and further cultivated for 4 h. The cells were

harvested by centrifugation at 15,000 rpm for 5 min at 4°C. After the cells were lysed using Bugbuster protein extraction reagent (Novagen), the inclusion bodies were isolated by centrifugation at 15,000 rpm for 5 min at 4°C and analyzed by Tricine-SDS PAGE. The intensity of Crp4 bands was quantified by densitometry.

Oxidative folding of chemically synthesized Crp4

Crp4 synthesized by Fmoc chemistry (Sigma-Aldrich Japan) was dissolved at 2 mg/ml in 50 mM Gly-NaOH buffer (pH 9.0) containing various concentrations of urea (0, 2, 4, 6 and 8 M). A 50 μl aliquot was withdrawn at different time intervals (0, 2, 4, 8 and 12 h). Then, the samples were acidified by 0.1% TFA to quench the folding reaction and injected into HPLC. HPLC analysis was performed on a Cosmosil 5C18-AR-300 column (Nacalai Tesque) using a linear gradient of 20-40% acetonitrile containing 0.1% TFA at a flow rate of 1 ml/min over 40 min. The folding yields were calculated by dividing the integrated area of the correctly folded Crp4 peak by the sum of the integrated area of all peaks.

Expression and inclusion body isolation for large scale production

The *E. coli* strain BL21(DE3) harboring the pCOLA-[Cys-less HLA]-Crp4 vector was cultured overnight at 37°C in 50 mL of medium (LB or M9) containing 20 μg/mL kanamycin. This preculture was inoculated into 1 L of medium (LB or M9) containing 20 μg/mL kanamycin. ^{15}N labeling was achieved by growing *E. coli* in M9 medium containing $^{15}NH_4Cl$ as the sole nitrogen source. The culture was grown at 37°C, and protein expression was induced by the addition of 1 mM IPTG when the OD600 reached 1.0-1.2. After an additional 4 h of cultivation, cells were harvested by centrifugation at 6,000 rpm for 10 min. The cells were resuspended in lysis buffer (50 mM Gly-NaOH, 1 mM EDTA, pH 9.0) and disrupted by sonication. Next, inclusion bodies composed mainly of Cys-less HLA and Crp4 were isolated by centrifugation at 7,500 rpm for 30 min at 4°C. The inclusion bodies

were washed twice with lysis buffer containing 0.1% TritonX-100 and washed once with lysis buffer (without TritonX-100).

Conventional refolding method with a reducing step

The procedure of the conventional refolding method is described in Figure 2. The washed inclusion bodies were solubilized in solubilization buffer (6 M urea, 50 mM Gly-NaOH, 3 mM EDTA, 200 mM β-mercaptoethanol, pH 9.0) to prepare completely reduced, unfolded Crp4. After centrifugation at 7,500 rpm at 4°C for 30 min, the clarified supernatant was loaded onto a HiTrap SP HP cation-exchange column (GE Healthcare) pre-equilibrated with equilibration buffer (6 M urea, 50 mM Gly-NaOH, 3 mM EDTA, 20 mM β-mercaptoethanol, pH 9.0). The bound Crp4 was eluted with a linear gradient of equilibration buffer with 0-1 M NaCl. The fractions containing Crp4 were identified using Tricine-SDS PAGE. These fractions were collected and dialyzed twice against refolding buffer (50 mM Gly-NaOH, 3 mM reduced glutathione, 0.3 mM oxidized glutathione, pH 9.0) for 12 h at 4°C. Next, the sample was dialyzed twice against 0.1% acetic acid for 12 h at 4°C. Correctly folded Crp4 was purified by RP-HPLC on a Cosmosil 5C18-AR-300 column (Nacalai Tesque). The elution was carried out with a linear gradient of 20-40% acetonitrile with 0.1% trifluoracetic acid. The yield of Crp4 was determined by measuring the absorbance at 280 nm. The purified recombinant Crp4 was lyophilized and stored at -30°C.

Direct refolding method without a reducing step

An experimental flowchart for the new method is shown in Figure 2. The washed inclusion bodies were solubilized in solubilization buffer without reducing agent (6 M urea, 50 mM Gly-NaOH, 3 mM EDTA, pH 9.0) and incubated for 12 h at 37°C in a shaker incubator to enhance oxidative folding of Crp4. After centrifugation at 7,500 rpm at 4°C for 30 min, the

clarified supernatant was loaded onto a HiTrap SP HP cation-exchange column (GE Healthcare) pre-equilibrated with equilibration buffer (6 M urea, 50 mM Gly-NaOH, 3 mM EDTA, pH 9.0). The bound Crp4 was eluted with a linear gradient of equilibration buffer with 0-1 M NaCl. The fractions containing Crp4 were identified using Tricine-SDS PAGE. These fractions were collected and dialyzed twice against 0.1% acetic acid for 12 h at 4°C. The HPLC purification was performed using the same method as described above.

Acid-urea polyacrylamide gel electrophoresis analysis

Acid-urea polyacrylamide gel electrophoresis (AU-PAGE) was performed basically according to the previously described method [30]. Prior to loading on a gel, an aliquot from each purification step was diluted in 3 × AU-PAGE sample buffer (9 M urea, 5% acetic acid, methyl green). For the analysis of Crp4 in inclusion bodies, inclusion bodies isolated from *E. coli* were directly solubilized into 3 × AU-PAGE sample buffer and then diluted in 5% acetic acid to prevent the formation of disulfide bonds of Crp4 during inclusion body solubilization. These samples were electrophoresed on 12.5% acrylamide gel containing 5% acetic acid and 5 M urea at 150 V. After electrophoresis, the gel was stained with Coomassie blue.

Bactericidal peptide assay of Crp4

Refolded Crp4 was tested for microbicidal activity against *E. coli* ML35 and *Listeria monocytogenes* (*L. monocytogenes*). The bacteria were cultured in the following media: *E. coli* ML35, tryptic soy broth; *L. monocytogenes*, brain heart infusion (BHI). Bacteria growing exponentially at 37°C were deposited by centrifugation at 9,300 g at 4°C for 5 min. Next, the bacteria were washed in 10 mM sodium phosphate buffer (pH 7.4) supplemented with a 0.01 volume of the culture medium and resuspended in the same buffer. The bacteria (~5×10^6 CFU/ml) were then incubated with recombinant Crp4 in 50 μl for 1 h in a shaker

incubator at 37°C, and the surviving bacteria were counted as CFU/ml after overnight growth on tryptic soy agar plates for *E. coli* ML35 and BHI agar plates for *L. monocytogenes*.

NMR spectroscopy

Recombinant Crp4 refolded during inclusion body solubilization was dissolved in a mixture of 90% H_2O/10% D_2O and adjusted to pH 4.2 by the addition of minute amounts of HCl or NaOH. NMR experiments were performed on a Bruker Avance III HD 600 MHz spectrometer. The HSQC spectrum was collected at 30°C. The data were processed processed using NMRPipe 4.1 [31] and analyzed using Sparky 3.113 software [32].

2-4 Results

Effect of coexpression of HLA and Cys-less HLA on the Crp4 expression level

To avoid enzymatic and chemical cleavage of fusion proteins, I tried to directly produce Crp4 in *E. coli* as an inclusion body. However, the expression level of Crp4 was extremely low (Fig. 3). Therefore, to enhance the inclusion body formation by Crp4, I applied the coexpression method.

In a previous study, I experimentally demonstrated that the inclusion body formation of a cationic antimicrobial peptide was enhanced by coexpression with an anionic partner protein [29]. Therefore, I chose an anionic partner protein, HLA, as a coexpression partner. The results showed that the expression of Crp4 was moderately increased by the coexpression of Crp4 and HLA.

Moreover, in this study, I evaluated the effect of Cys residues of HLA on the inclusion body formation of Crp4 by using Cys-less HLA, in which all eight Cys residues were converted to Ser residues. The expression of Crp4 was markedly increased as an inclusion body by coexpression of Cys-less HLA (Fig. 3). Because the expression level of Crp4 was most increased by coexpression of Cys-less HLA, I selected Cys-less HLA as a partner protein for the large-scale production of Crp4.

Oxidative folding of chemically synthesized Crp4

To obtain a large amount of correctly folded Crp4, it is important to determine the best condition for refolding of Crp4. It has been reported that human α-defensins folded efficiently in the presence of a proper quantity of denaturant [33]. Therefore, I examined the folding behavior of chemically synthesized Crp4 under denaturing conditions. Moreover, I evaluated the effect of the concentration of urea on the refolding yield of Crp4. As shown in Figure 4, the optimal concentration of urea is 2 M, yielding a 35.4% recovery after 12 h at

room temperature. Similarly, in the presence of 4 M urea, the refolding yield after 12 h was 34.0%. As the concentration of urea increased from 4 M to 8 M, the refolding yield gradually declined. Also under non-denaturing conditions, Crp4 folded correctly, although at a ,much slower rate. No aggregation of Crp4 was observed under any of the experimental conditions employed.

Purification and refolding of Crp4 by using a conventional refolding method with a reducing step

Because Crp4 has a charge that is opposite that of Cys-less HLA, I succeeded in separating Crp4 from Cys-less HLA efficiently by a simple one-step cation-exchange chromatography without enzymatic or chemical cleavage (Fig. 5a). After cation-exchange chromatography, I obtained 12 mg of reduced recombinant Crp4. Then, this crude Crp4 was refolded by a simple standard dialysis refolding protocol (Fig. 2). From the results of refolding analysis using chemically synthesized Crp4, I refolded Crp4 in the presence of 2 M urea. After the refolding and purification procedure, I obtained 2.0 mg of correctly folded Crp4 from 1 L of culture. Although I succeeded in obtaining milligram quantities of correctly folded Crp4 by using a conventional method with a reducing agent, a large amount of Crp4 precipitate was observed after the refolding process.

Purification and refolding of Crp4 using the new method without a reducing step

To enhance the refolding yield of Crp4 and avoid the cumbersome refolding step, I attempted to refold Crp4 directly during inclusion body solubilization. Because I expected that the omission of reducing agent from the solubilization buffer would lead to the disulfide bridge formation of Crp4, I attempted to solubilize inclusion bodies of Crp4 in the solubilization buffer without reducing agent. Although I demonstrated that chemically synthesized Crp4 could be folded efficiently in the presence of 2-4 M urea, the inclusion

body was not solubilized in 2-4 M urea (data not shown). Therefore, the inclusion body was solubilized in solubilization buffer containing 6 M urea. Refolding of Crp4 during inclusion body solubilization was examined by AU-PAGE analysis. Because small cationic peptides are separated on the basis of both the molecular size and charge, AU-PAGE is a suitable method for evaluating the homogeneity and formation of native structure of defensins. In the case that the isolated inclusion body was directly solubilized in acidic AU PAGE buffer (approximately pH 3), the mobility of Crp4 was equal to that of reduced chemically synthesized Crp4, suggesting that no disulfide bridges were formed (Fig 5b). In contrast, the mobility of Crp4 after 12 h solubilization using solubilization buffer (pH 9.0) without reducing agent was clearly different from that of reduced Crp4. Moreover, the mobility of Crp4 was not changed during the following purification step. These results indicated that the disulfide bridge formation of Crp4 did not occur in E. coli cells but was completed during inclusion body solubilization without a reducing agent. Aggregation of Crp4 was not confirmed after the refolding process. After HPLC purification, I obtained 4.6 mg of correctly folded Crp4 from 1 L of culture.

Antimicrobial activity of recombinant Crp4

The microbicidal activity of refolded Crp4 was examined by colony count assay (Fig. 6). The purified Crp4 was active against both *E. coli* ML35 and *L. monocytogenes*. Moreover, the Gram-negative bacterium (*E. coli* ML35) was more sensitive than the Gram-positive bacterium (*L. monocytogenes*). These results were in accordance with the findings reported previously [10].

TOCSY and HSQC spectrum of Crp4

To confirm that the Crp4 refolded by new refolding method had the correct structure, the TOCSY and HSQC spectra of Crp4 were obtained. The fingerprint region of the TOCSY

spectrum is presented in Figure 7. I confirmed that the chemical shift of the side chain amide proton of Arg7 was shifted markedly downfield. Such a shift was also reported in the previous study [8]. Moreover, the spectrum was quite similar to that observed in the previous study. These results indicate that the Crp4 refolded during inclusion body solubilization had the correct structure. In addition, I could easily prepare isotopically labeled Crp4 due to the good expression efficiency. The HSQC spectrum of ^{15}N-labeled Crp4 is presented in Figure 8. The well-dispersed peaks in HSQC also indicate that Crp4 was correctly folded. Sequential specific ^{1}H and ^{15}N resonance assignments were also determined without any ambiguity.

2-5 Discussion

In this study, I chose a mouse α-defensin, Crp4, as the target peptide. To avoid enzymatic or chemical cleavage of the fusion protein, I at first tried to express Crp4 directly in *E. coli*. Unfortunately, the direct expression of Crp4 in *E. coli* was insufficient, probably due to the instability of the expressed cellular Crp4 itself (Fig. 3). I speculated that this low-level expression of Crp4 was caused by the degradation of expressed Crp4 by proteases of *E. coli*. Therefore, I decided to apply a previously developed method [29], which enhances the inclusion body formation of the target peptide by coexpression of aggregation-prone protein as a partner protein, for overexpression of Crp4.

In my previous study, I examined the effect of the charge of the partner protein on the inclusion body formation by the target peptide via this method and concluded that the opposite charge of the partner protein efficiently enhanced the formation of an inclusion body of the target peptide [29]. In this study, because Crp4 is a cationic antimicrobial peptide (pI 9.9), I selected anionic HLA (pI 4.7) as a candidate for the coexpression partner protein for overexpression of Crp4. To further elucidate the mechanism of inclusion body formation by the target peptide via this method, I evaluated the effect of Cys residues of the partner protein on the inclusion body formation by the target peptide using Cys-less HLA.

Similarly to HLA, Cys-less HLA formed a large amount of inclusion bodies when overexpressed in *E. coli* (Fig. 3a). This result was consistent with earlier findings that a mutant of HLA, in which all eight Cys residues are substituted to Ala residues, forms inclusion bodies in *E. coli* [34], although in my study the Cys residues of HLA were mutated to Ser residues. From these results, it can be said that the Cys mutations of HLA did not affect the propensity to form inclusion bodies in *E. coli*. Interestingly, while coexpression of HLA modestly enhanced the expression level of Crp4, Crp4 was produced effectively as an inclusion body in the case of coexpression with Cys-less HLA. In this

study, I could not clarify why Cys-less HLA induced a greater increase in the expression level of Crp4 than HLA.

To enhance the refolding yield of Crp4, I focused on previous studies which showed that proteins in inclusion bodies have a native-like secondary structure, and the restoration of this native-like structure using mild solubilization conditions promotes refolding of the proteins [35]. Unfortunately, in the present study the inclusion bodies that mainly contained Crp4 and Cys-less HLA were not solubilized under a mild condition (2-4 M urea). However, I were able to confirm that chemically synthesized Crp4 was also refolded even in the presence of a high concentration of urea (6-8 M urea). Therefore, I expected that the refolding of Crp4 without a complete denaturing step would enhance the refolding yield of Crp4. I therefore tried to apply my present method to induce Crp4 to form disulfide bridges during the solubilization of inclusion bodies (Fig. 2). In this method, to facilitate disulfide bridge formation of Crp4 during inclusion body solubilization, I removed the reducing agent from the inclusion body solubilization buffer. As a result, I succeeded in the refolding of Crp4 during inclusion body solubilization and obtaining 4.6 mg of correctly folded Crp4 after HPLC purification. I also tried to refold Crp4 during the solubilization of inclusion bodies mainly composed of Crp4 and HLA (Cys-containing), but the refolding of Crp4 was inhibited by intermolecular disulfide bridge formation between Crp4 and HLA (data not shown). From these results, it can be said that the coexpression of Cys-less HLA is effective not only to enhance the expression of Crp4 as inclusion bodies but also to prevent the interruption of refolding of Crp4 during inclusion body solubilization caused by the formation of intermolecular disulfide bridges.

In order to avoid the degradation of recombinant proteins and peptides by host-derived proteases in and after the refolding step, partially purified proteins and peptides are generally used as starting materials for the in vitro refolding of inclusion body. In this study, I confirmed that Crp4 has the ability to refold efficiently in the presence of a proper

concentration of urea (Fig. 4). Under these conditions, host-derived proteases are thought to be denatured. This may be the reason why the yield of correctly folded Crp4 obtained by the direct refolding method was high even without partial purification.

Unlike in the conventional fusion protein system, there is no need to remove the fusion protein tag by enzymatic or chemical methods in my coexpression method. Therefore, my coexpression system can be applied to the production of any α-defensin. In future studies, I plan to use this method to produce α-defensins that are difficult to synthesize by conventional fusion protein methods.

Table 1. Sequence of primers used in this study

Name	Primer sequence[a] (from the 5' end to 3' end)	Restriction site
Primers for the Crp4 gene	F = GGAATTCCATATGGACATCG ACTTTAGTACTTGTGC	*Nde*I
	R = CCGCTCGAGTCAGCGGCGGG GG	*Xho*I
Primers for the HLA gene	F = GAATTCTCATGAAGCAATTC ACAAAATGTGAGCTG	*Nco*I
	R = CGGGATCCTTACAACTTCTC ACAAAGCCACTG	*Bam*HI
Primers for the Cys-less HLA gene	F = GAATTCCCATGGGCAAGCAA TTCACAAAATCTGAG	*Nco*I
	R = CGGGATCCTTACAACTTCTC AGAAAGCCAC	*Bam*HI

a. Restriction sites are underlined.

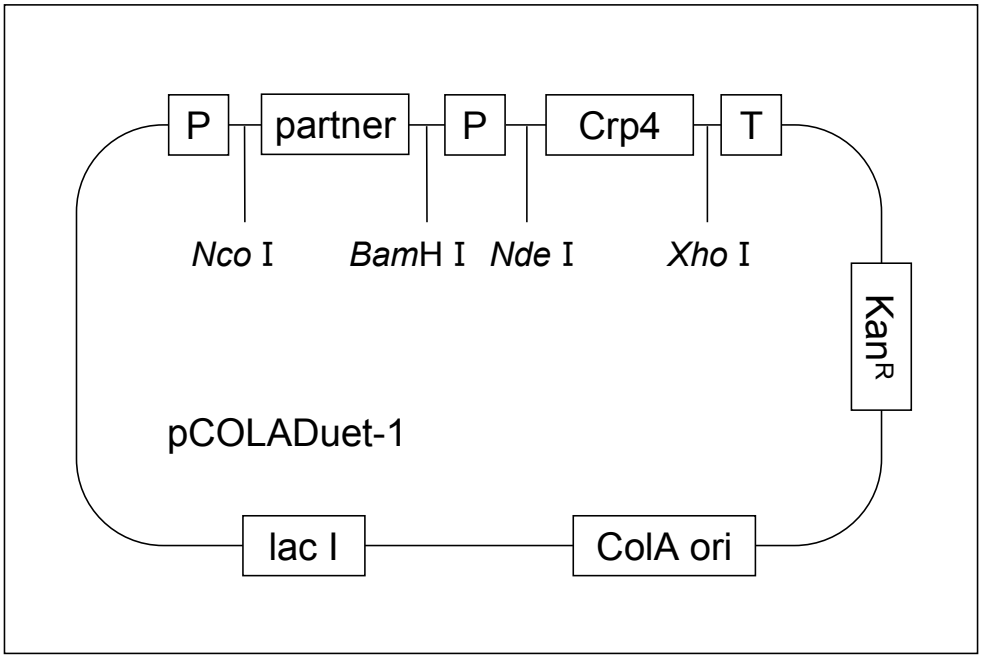

Figure 1. Schematic representation of the expression vector. P, T7 promoter; partner, partner protein gene; Crp4, Crp4 gene; T, T7 terminator.

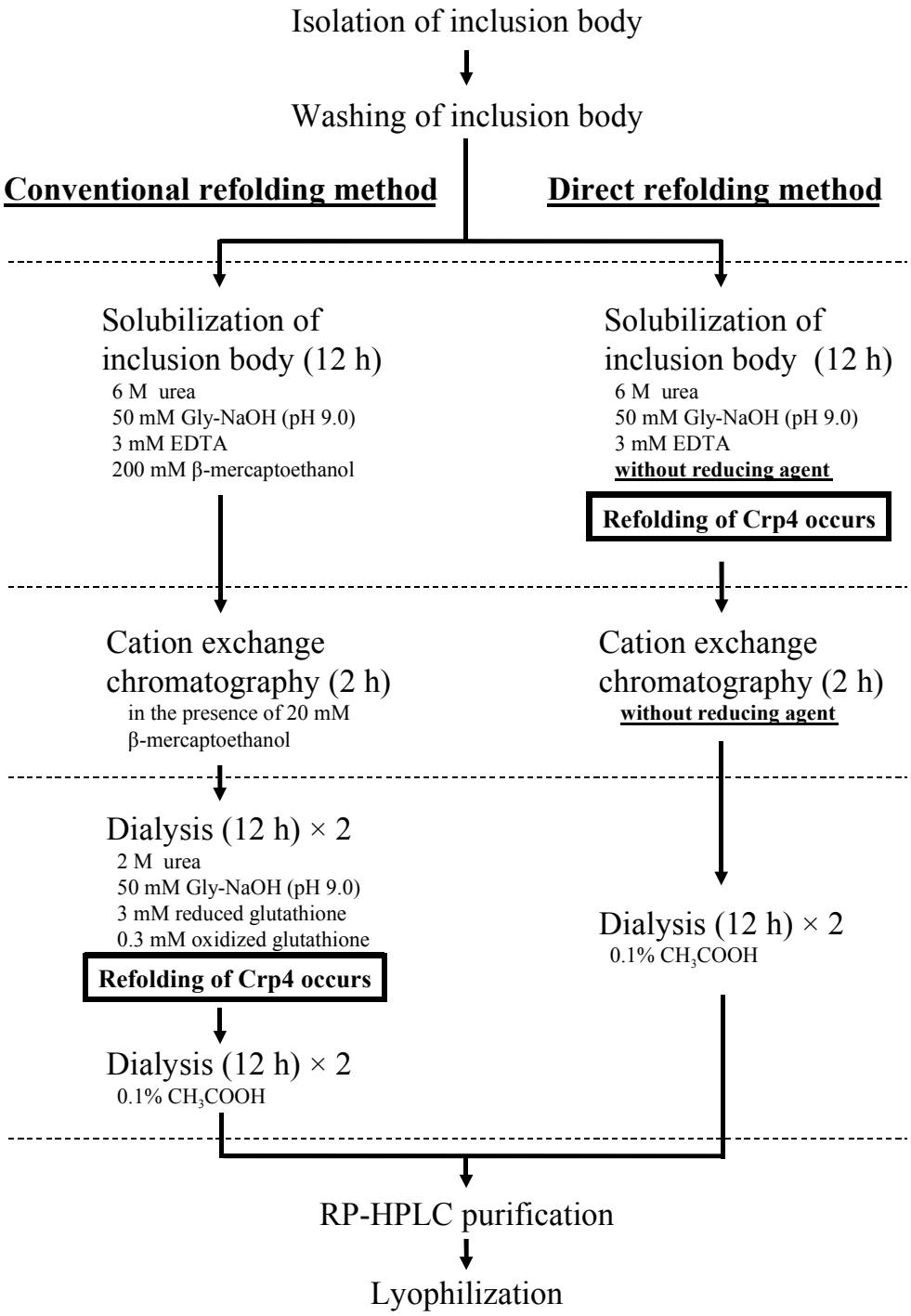

Figure 2. Comparison of the conventional refolding method and the direct refolding method without a reducing step. Flowcharts are given for the conventional method (left) and the direct refolding method (right). The time point of Crp4 refolding, the presence or absence of reducing agent, and the time required for each step are shown.

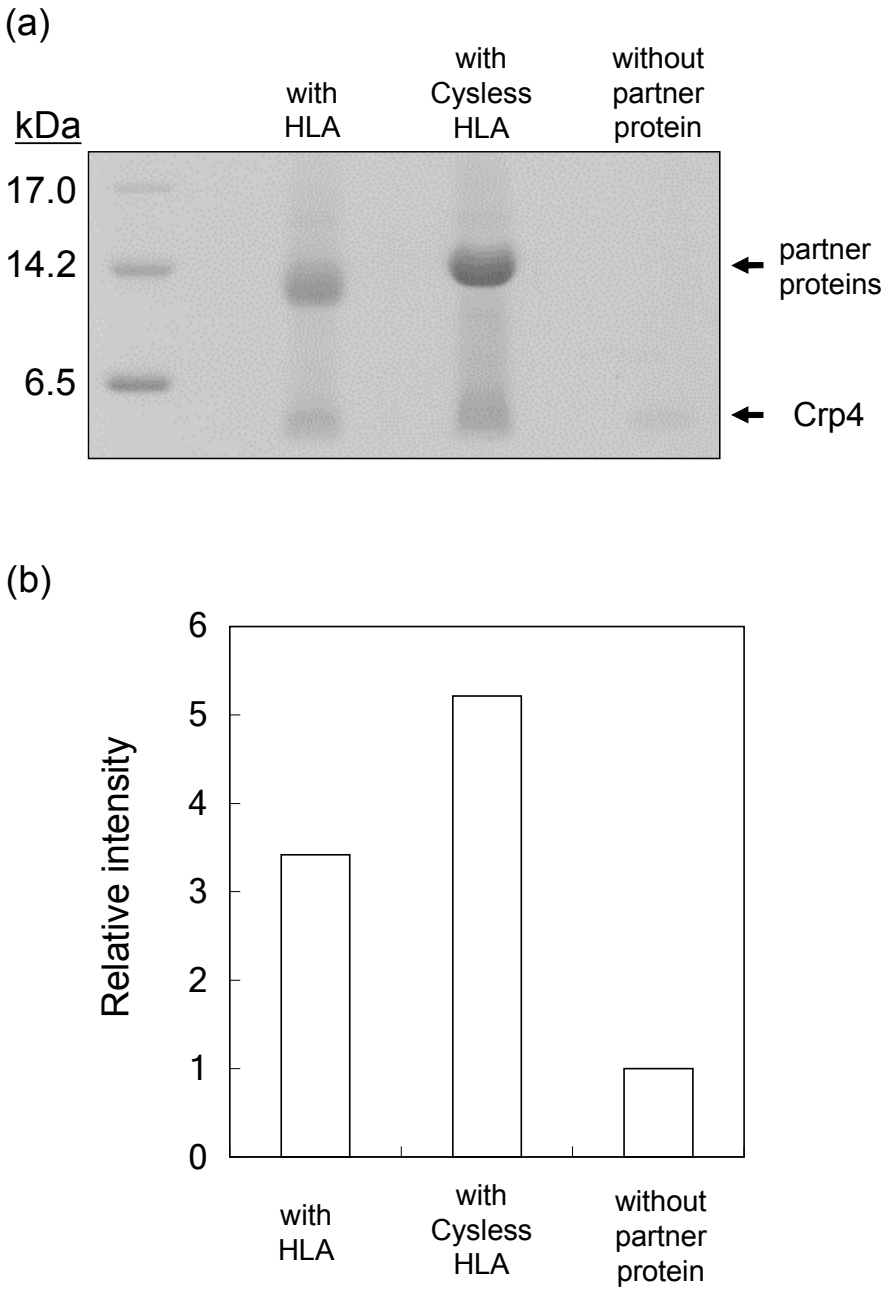

Figure 3. Effect of the Cys residues of HLA on Crp4 expression level. (a) Tricine-SDS-PAGE analysis of the expression level of Crp4. (b) The intensity data of the coexpression method are expressed in relation to those for the direct expression method.

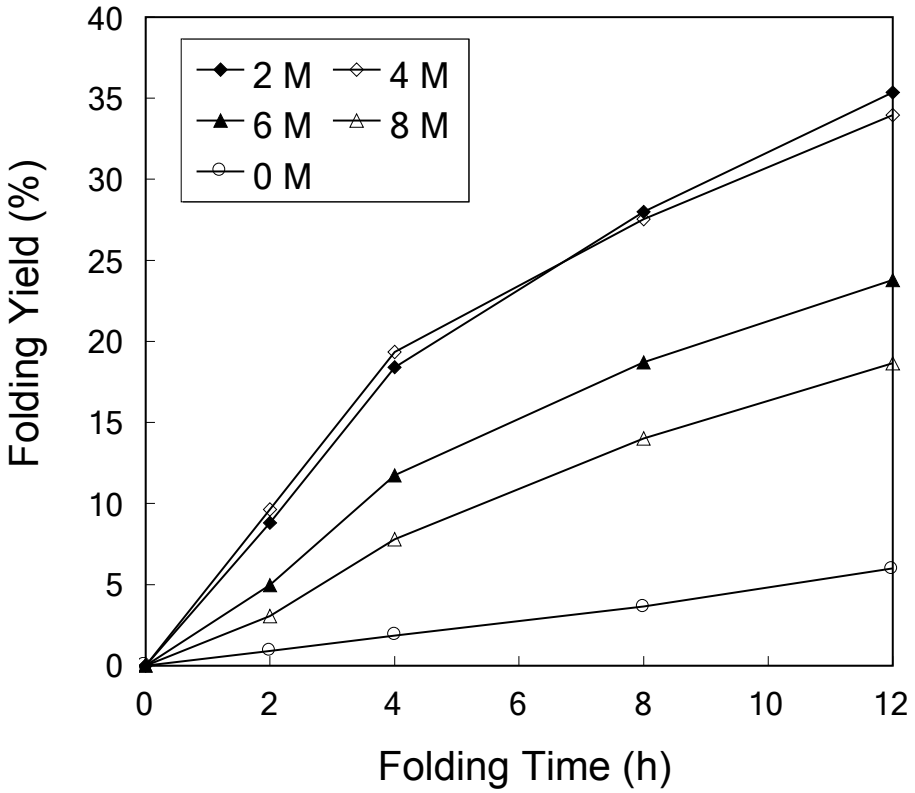

Figure 4. Time dependence of the folding yields for chemically synthesized Crp4 under different urea concentrations.

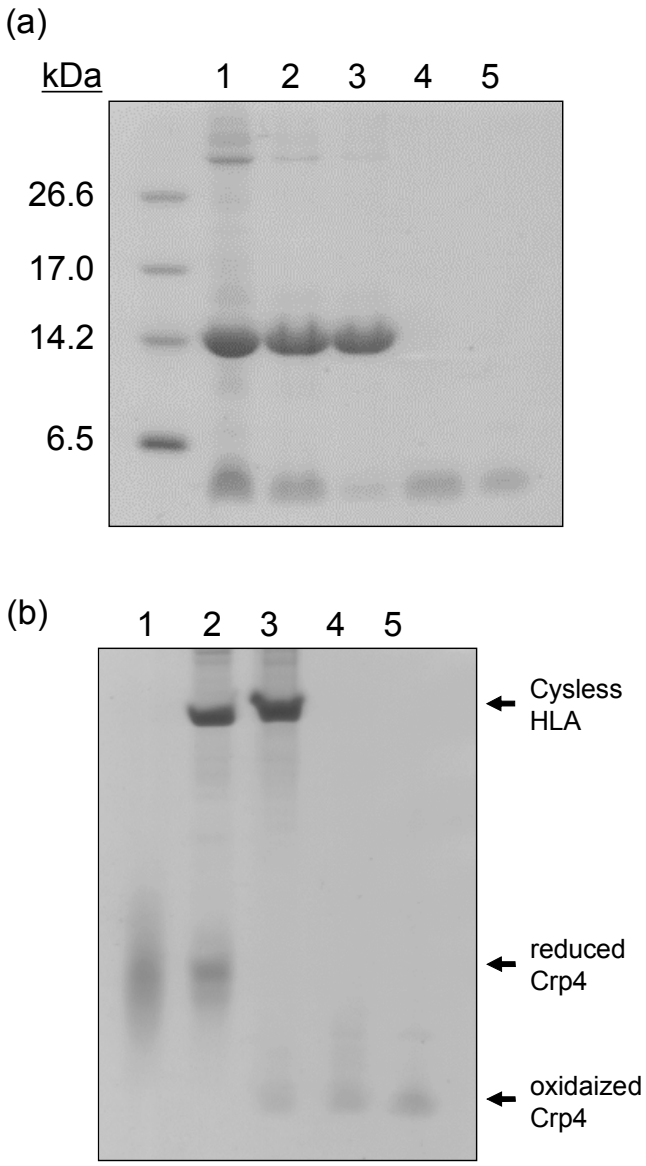

Figure 5. Expression and purification of recombinant Crp4. Tricine-SDS PAGE (a) and AU-PAGE (b) analysis of Crp4. (a) Lane 1: Inclusion body after ultrasonication and centrifugation. Lane 2: Solubilized inclusion body. Lane 3: A flowthrough fraction that was passed through cation-exchange chromatography. Lane 4: Purified Crp4 using cation-exchange chromatography. Lane 5: Purified correctly folded Crp4 using RP-HPLC. (b) Lane 1: Chemically synthesized reduced Crp4. Lane 2: Inclusion body solubilized in AU-PAGE buffer (approximately pH 3). Lane 3: Inclusion body after 12 h solubilization in solubilization buffer (pH 9.0). Lane 4: Purified correctly folded Crp4 using cation-exchange chromatography. Lane 5: Purified correctly folded Crp4 using RP-HPLC.

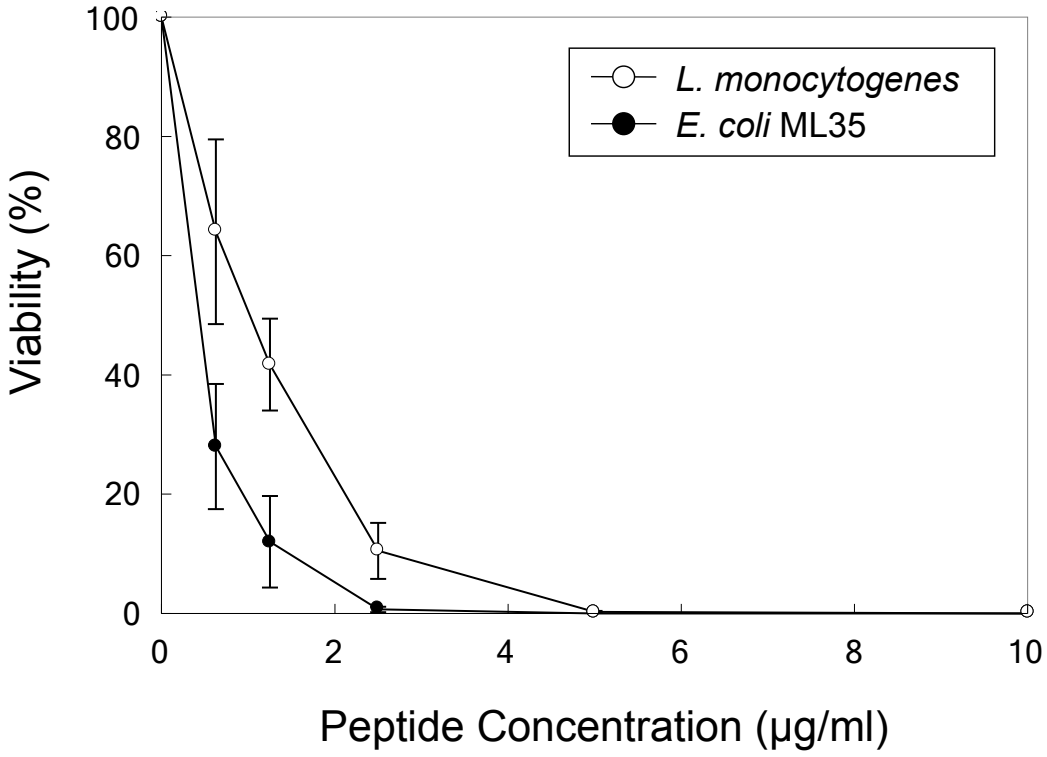

Figure 6. Bactericidal activity of Crp4 refolded by using the direct refolding method.

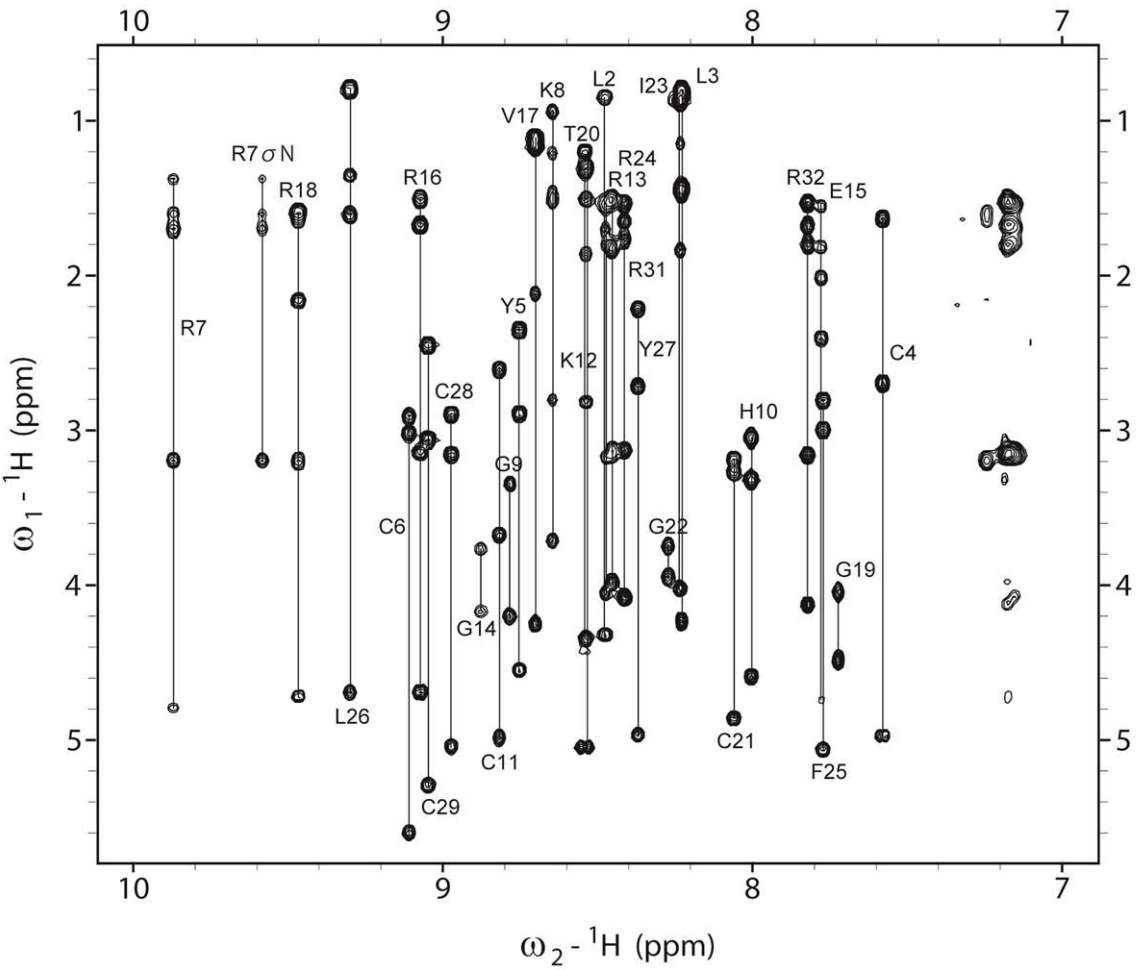

Figure 7. Fingerprint region of the 2D TOCSY spectrum of Crp4.

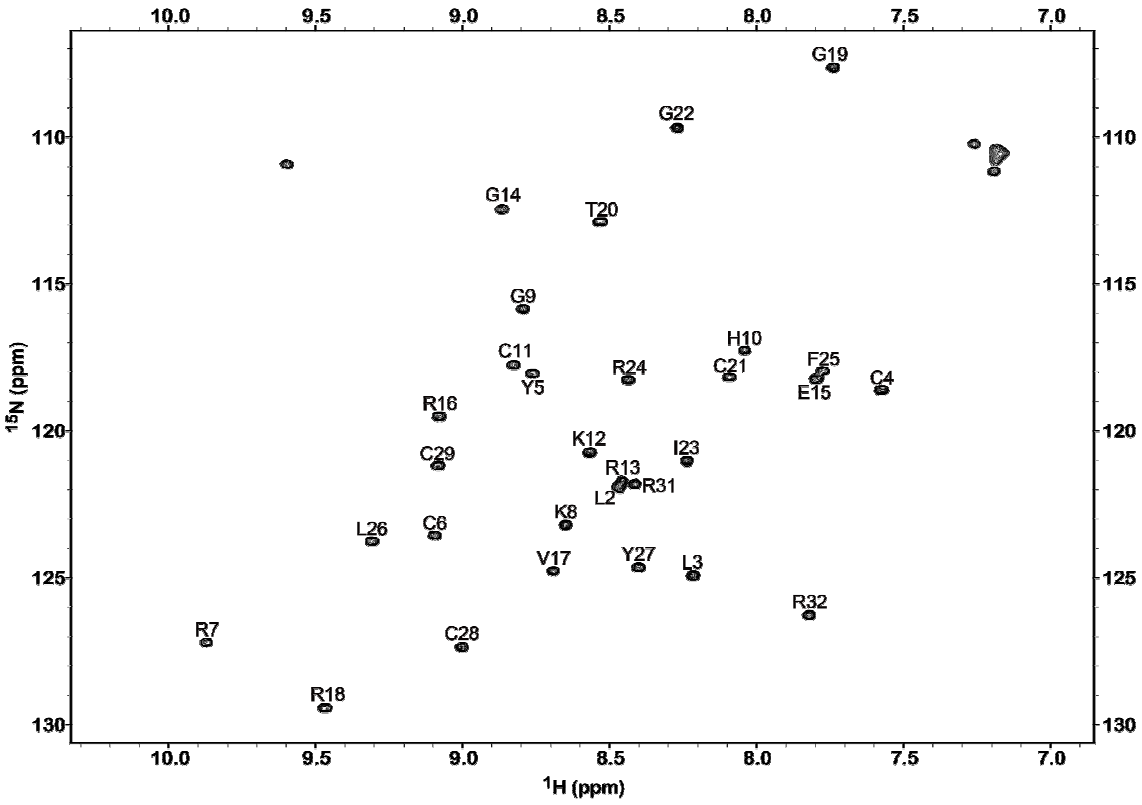

Figure 8. ^{1}H-^{15}N HSQC spectrum of 0.5 mM ^{15}N-labeled Crp4.

2-6 References

[1] H.G. Boman, Innate immunity and the normal microflora, Immunol. Rev. 173 (2000) 5-16.

[2] E. Guaní-Guerra, T. Santos-Mendoza, S.O. Lugo-Reyes, L.M. Terán, Antimicrobial peptides: General overview and clinical implications in human health and disease, Clin. Immunol. 135 (2010) 1-11.

[3] M.E. Selsted, A.J. Ouellette, Mammalian defensins in the antimicrobial immune response. Nat. Immunol. 6 (2005) 551-557.

[4] R.I. Lehrer, T. Ganz, Defensins of vertebrate animals, Curr. Opin. Immunol. 14 (2002) 96-102.

[5] J. Jarczak, E.M. Kościuczuk, P. Lisowski, N. Strzałkowska, A. Jóźwik, J. Horbańczuk, J. Krzyżewski, L. Zwierzchowski, E. Bagnicka, Defensins: Natural component of human innate immunity, Hum. Immunol. 74 (2013) 1069-1079.

[6] T Ayabe, D.P. Satchell, C.L. Wilson, W.C. Parks, M.E. Selsted, A.J. Ouellette, Secretion of microbicidal alpha-defensins by intestinal Paneth cells in response to bacteria, Nat. Immunol. 1 (2000) 113-118.

[7] A.J. Ouellette, M.M. Hsieh, M.T. Nosek, D.F. Cano-Gauci, K.M. Huttner, R.N. Buick, M.E. Selsted, Mouse Paneth cell defensins: primary structures and antibacterial activities of numerous cryptdin isoforms, Infect. Immun. 62 (1994) 5040-5047.

[8] W. Jing, H.N. Hunter, H. Tanabe, A.J. Ouellette, H.J. Vogel, Solution structure of

cryptdin-4, a mouse paneth cell alpha-defensin, Biochemistry 43 (2004) 15759-15766.

[9] K.J. Rosengren, N.L. Daly, L.M. Fornander, L.M. Jönsson, Y. Shirafuji, X. Qu, H.J. Vogel, A.J. Ouellette, D.J. Craik, Structural and functional characterization of the conserved salt bridge in mammalian paneth cell alpha-defensins: solution structures of mouse CRYPTDIN-4 and (E15D)-CRYPTDIN-4, J. Biol. Chem. 281 (2006) 28068-28078.

[10] A. Maemoto, X Qu, K.J. Rosengren, H. Tanabe, A. Henschen-Edman, D.J. Craik, A.J. Ouellette, Functional analysis of the α-defensin disulfide array in mouse cryptdin-4, J. Biol. Chem. 279 (2004) 44188-44196.

[11] C. Hadjicharalambous, T. Sheynis, R. Jelinek, M.T. Shanahan, A.J. Ouellette, E. Gizeli, Mechanisms of alpha-defensin bactericidal action: comparative membrane disruption by Cryptdin-4 and its disulfide-null analogue, Biochemistry 47 (2008) 12626-12634.

[12] H. Tanabe, X Qu, C.S. Weeks, J.E. Cummings, S. Kolusheva, K.B. Walsh, R. Jelinek, T.K. Vanderlick, M.E. Selsted, A.J. Ouellette, Structure-activity determinants in paneth cell alpha-defensins: loss-of-function in mouse cryptdin-4 by charge-reversal at arginine residue positions, J. Biol. Chem. 279 (2004) 11976-11983.

[13] H.S. Andersson, S.M. Figueredo, L.M. Haugaard-Kedström, E. Bengtsson, N.L. Daly, X. Qu, D.J. Craik, A.J. Ouellette, K.J. Rosengren, The α-defensin salt-bridge induces backbone stability to facilitate folding and confer proteolytic resistance, Amino Acids 43 (2012) 1471-1483.

[14] R.A. Llenado, C.S. Weeks, M.J. Cocco, A.J. Ouellette, Electropositive charge in alpha-defensin bactericidal activity: functional effects of Lys-for-Arg substitutions vary with the peptide primary structure, Infect. Immun. 77 (2009) 5035-5043.

[15] N.W. Schmidt, K.P. Tai, K. Kamdar, A. Mishra, G.H. Lai, K. Zhao, A.J. Ouellette, G.C. Wong, Arginine in α-defensins: differential effects on bactericidal activity correspond to geometry of membrane curvature generation and peptide-lipid phase behavior, J. Biol. Chem. 287 (2012) 21866-21872.

[16] N.F. Dawson, D.J. Craik, A.M. Mcmanus, S.G. Dashper, E.C. Reynolds, G.W. Tregear, L.O. JR, J.D. Wade, Chemical synthesis, characterization and activity of RK-1, a novel alpha-defensin-related peptide, J. Pept. Sci. 6 (2000) 19-25.

[17] P.A. Raj, K.J. Antonyraj, T. Karunakaran, Large-scale synthesis and functional elements for the antimicrobial activity of defensins, Biochem. J. 347 (2000) 633-641.

[18] Z. Wu, B. Ericksen, K. Tucker, J. Lubkowski, W. Lu, Synthesis and characterization of human α-defensins 4-6, J. Pept. Res. 64 (2004) 118-125.

[19] E. Vernieri, J. Valle, D. Andreu, B.G. de la Torre, An optimized Fmoc synthesis of human defensin 5, Amino Acids 46 (2014) 395-400.

[20] M. Pazgier, J. Lubkowski, Expression and purification of recombinant human α-defensins in *Escherichia coli*, Protein Expression Purif. 49 (2006) 1-8.

[21] O. Bruhn, P. Regenhard, M. Michalek, S. Paul, C. Gelhaus, S. Jung, G. Thaller, R.

Podschun, M. Leippe, J. Grötzinger, E. Kalm, A novel horse α-defensin: gene transcription, recombinant expression and characterization of the structure and function, Biochem. J. 407 (2007) 267-276.

[22] A. Wang, Y. Su, S. Wang, M. Shen, F. Chen, M. Chen, X. Ran, T. Cheng, J. Wang, High efficiency preparation of bioactive human α-defensin 6 in *Escherichia coli* Origami(DE3)pLysS by soluble fusion expression, Appl. Biochem. Biotechnol. 87 (2010) 1935-1942.

[23] N. Chapnik, A. Levit, M.Y. Niv, O. Froy, Expression and structure/function relationships of human defensin 5, Appl. Biochem. Biotechnol. 166 (2012) 1703-1710.

[24] A Wang, S. Wang, M. Shen, F. Chen, Z. Zou, X. Ran, T. Cheng, Y. Su, J. Wang, High level expression and purification of bioactive human α-defensin 5 mature peptide in *Pichia pastoris*, Appl. Microbiol. Biotechnol. 84 (2009) 877-884.

[25] K.H. Hsu, C. Pei, J.Y. Yeh, C.H. Shih, Y.C. Chung, L.T. Hung, B.R. Ou, Production of bioactive human α-defensin 5 in *Pichia pastoris*, J. Gen. Appl. Microbiol. 55 (2009) 395-401.

[26] W. Cao, Y. Zhou, Y Ma, Q. Luo, D. Wei, Expression and purification of antimicrobial peptide adenoregulin with C-amidated terminus in *Escherichia coli*, Protein Expr. Purif. 40 (2005) 404-410.

[27] Y. Yang, Z. Tian, D. Teng, J. Zhang, J. Wang, J. Wang, High-level production of a

candidacidal peptide lactoferrampin in *Escherichia coli* by fusion expression, J. Biotechnol. 139 (2009) 326-331.

[28] M. Zorko, R. Jerala, Production of recombinant antimicrobial peptides in bacteria, Methods Mol Biol, 618 (2010) 61-76.

[29] S. Tomisawa, E. Hojo, Y. Umetsu, Y. Kato, M. Miyazawa, M. Mizuguchi, M. Kamiya, Y. Kumaki, T. Kikukawa, M. Demura, T. Aizawa, Overexpression of an antimicrobial peptide derived from *C. elegans* using an aggregation-prone protein coexpression system, AMB Express 3 (2013) 45.

[30] S. Figueredo, J.R. Mastroianni, K.P. Tai, A.J. Ouellette, Expression and Purification of Recombinant α-Defensins and α-Defensin Precursors in *Escherichia coli*, Methods Mol. Biol. 618 (2010) 47-60.

[31] F. Delaglio, S. Grzesiek, G.W. Vuister, G. Zhu, J. Pfeifer, A. Bax, NMRPipe: A multidimensional spectral processing system based on UNIX pipes, J. Biomol. NMR 6 (1995) 277-293.

[32] T.D. Goddard, D.G. Kneller, SPARKY 3 software, University of California, San Francisco, USA (2006).

[33] Z. Wu, R. Powell, W. Lu, Productive folding of human neutrophil α-defensins in vitro without the pro-peptide, JACS 125 (2003) 2402-2403.

[34] Z. Peng, L.C. Wu, P.S. Kim, Local structural preferences in. the α-lactalbumin molten

globule, Biochemistry 34 (1995) 3248-3252.

[35] S.M. Singh, A.K. Panda, Solubilization and refolding of bacterial inclusion body proteins, J. Biosci. Bioeng. 99 (2005) 303-310.

Chapter 3

A new approach to detect small peptides clearly and sensitively by Western blotting using a vacuum-assisted detection method

3-1 Abstract

Western blotting is a widely used technique for the detection and quantification of proteins and peptides. However, it is challenging to detect small peptides efficiently by the conventional Western blotting method with shaking, in part because the peptides readily detach from the blotted membrane. Although some modified Western blotting protocols have been developed to overcome this problem, it remains difficult to prevent peptide detachment from the membrane. In this study, I show that the previously developed vacuum-assisted detection method greatly improves the detection of small peptides without additional protocol modification. The vacuum-assisted method was developed to shorten the time required for all immunodetection steps, and all the Western blotting solutions penetrated the membrane quickly and efficiently by this method. By using this vacuum method, I succeeded in detecting small peptides that were completely undetectable by the conventional Western blotting method. I also confirmed that peptide detachment was induced even by gentle shaking in the case of the conventional method, and the detachment was accelerated when detergent was present in the buffer. Unlike in the conventional method, there is no need to shake the membrane in solution in the vacuum method. Therefore, it is thought that the small peptides could be detected sensitively only by the vacuum method.

3-2 Introduction

Western blotting is a powerful procedure to identify and quantify low-abundance proteins and peptides. However, it is difficult to detect low-molecular-weight peptides efficiently, in part because they so readily detach from the blotted membranes. To avoid this detection problem, previous researchers have fixed the blotted membranes with aldehyde before applying them to the conventional Western blotting method with shaking [1-3]. Nishi *et al.* succeeded in detecting a low-molecular-weight (6 kDa) epidermal growth factor by fixation of a gelatin-coated PVDF membrane with formaldehyde. Lee *et al.* reported that fixation of a blotted membrane with paraformaldehyde enables clear and strong detection of endogenous α-synuclein (17 kDa). Although membrane fixation by this kind of chemical crosslinkers can improve the retention of peptides on the membrane, it has also been reported that such fixation can be affect the peptide immunoreactivity due to the chemical modification [4]. Therefore, it is very important to develop an alternative detection method that does not alter the immunoreactivity of peptides.

In this study, I demonstrated that the previously developed vacuum-assisted detection method greatly improved the retention of small peptides without the need to fix the blotted membranes. The length of time for immunodetection could be reduced by the vacuum method, since all the Western blotting solutions permeated the membrane

rapidly by this method. Because of this advantage, the vacuum method has been widely used to detect the protein of interest in many studies [5-7]. Two vacuum systems are commercially available for laboratory use, the SNAP i.d. system (Millipore) and the Western Q system (SciTrove). By using the vacuum method, I could detect small peptides that were not detectable by the conventional Western blotting method. In addition, I found that the multiple number of cysteine residues in peptides were related to the retention of the peptides on the membranes. The vacuum-assisted detection method was originally developed in order to shorten the time required for all immunodetection steps. To my knowledge there are no published data highlighting the detection of small peptides using the vacuum method. In this study, I assessed the effectiveness of the vacuum method for the detection of small peptides.

3-3 Materials and Methods

Biotinylated antibody and peptides

Six kinds of C-terminal biotinylated peptides (Table 1) were synthesized by Fmoc chemistry (Sigma-Aldrich Japan). A cysteine residue was introduced at the C-terminus of non-cysteine containing peptides (BLP7, MG2, CP1), and then the peptides were biotinylated with iodoacetamide-biotin. In addition, cysteine-containing peptides (TEWP, pBD2, TPI), which contained a C-terminal 2-aminoethylamide moiety, were prepared using ethylenediamine trityl resin. After the fully protected peptides were cleaved from the resin, biotin was coupled to the free amino group at the C-terminus. An anti-Salmonella antibody (a kind gift from the R&D Center, Nippon Meat Packers Inc.) was biotinylated by using a Biotin Protein Labeling Kit (Roche) according to the protocol provided by the supplier. This biotinylated polyvalent antibody was used as a positive control in the Western blotting.

Electrophoresis

Prior to loading on a gel, samples were diluted in 2 × sample buffer (100 mM Tris-HCl (pH 8.4), 24% glycerol, 1% SDS, 2% β-mercaptoethanol, 0.02% Coomassie G-250) and heated at 95˚C for 5 min. Tricine-SDS-polyacrylamide gel electrophoresis was performed using CPAGEL (ATTO) and Compact PAGE (twin) (AE7341, ATTO) by a previously described method [8]..

Electrotransfer

The transfer buffers used were formulated as follows. Cathode buffer consisted of 25 mM Tris, 40 mM 6-amino-n-hexanonic acid, and 5% methanol; anode buffer A consisted of 300 mM Tris and 5% methanol; anode buffer B was made up of 25 mM Tris and 5% methanol. Prior to electrotransfer, a PVDF membrane (6 cm × 6 cm)

(Immobilon-Psq, pore size 0.2 μm; Millipore) was treated with methanol for 20 s, transferred to a container of distilled water for 1 min, and then soaked with the anode buffer B for 30 min. After electrophoresis, the gels were equilibrated in anode buffer B for 5 min. The gel and membrane were sandwiched in the following order from bottom to top: three pieces of filter paper soaked with anode buffer A, a piece of filter paper soaked with anode buffer B, the pre-wetted membrane, the gel, and three pieces of filter paper soaked with cathode buffer. Electrotransfer was performed at a constant current of 54 A (1.5 mA/cm^2) for 40 min using a HorizBLOT 2M blotting unit (AE6687, ATTO).

Conventional shaking detection method

The procedure of the conventional method is described in Fig. 1. The blotted membrane was blocked with 30 mL of blocking buffer (StabilGuard Choice, SurModics) for 30 min and then washed with 30 mL of TBS-T (10 mM Tris HCl (pH 8.0), 150 mM NaCl, 0.1% Tween20) twice for 10 min with gentle shaking. After washing with TBS-T, the membrane was incubated at room temperature for 1 h with streptavidin horseradish peroxidase (HRP) conjugate (GE Healthcare) in 15 mL of blocking buffer; the dilution ratio was 1:1000. The membrane was then washed with 30 mL of TBS-T twice for 10 min with gentle shaking. The bound peptides and antibody were visualized by Clarity western substrate (Bio-Rad) according to the protocol provided by the supplier. The luminescent signals were acquired by using a cooled CCD camera system (AE-6971 Light Capture, ATTO).

Vacuum-assisted detection method

Detection with a SNAP i.d. vacuum system (Millipore) was performed basically according to the protocol provided by the supplier (Fig. 1). Briefly, after the blot holder containing the blotted membrane was placed in the SNAP i.d. vacuum system, 30 mL of blocking buffer was added and then the vacuum was turned on. After the well had emptied completely, the

vacuum was turned off. Next, Streptavidin HRP conjugate in 5 mL of blocking buffer (dilution ratio 1:333) was added into the blot holder. After incubation for 10 min, the vacuum was turned on and then the membrane was washed three times with 30 mL of TBS-T. The chemiluminescent reaction and detection were performed using the same method as described above.

The effect of Tween 20 on peptide retention

After electrophoresis, CP1 was electrotransferred from the gel to the pre-wetted membrane. The peptide was detected by a vacuum system as described above. The membrane was washed with TBS (10 mM Tris HCl (pH 8.0), 150 mM NaCl) for 10 s to remove the chemiluminescent reagent. The membrane was then washed again with TBS-T or TBS for 10 min with gentle shaking. The residual peptides were visualized and then the luminescent signals were acquired. These procedures were repeated four times.

3-4 Results

While all six peptides were clearly detected by the vacuum method, only three peptides were weakly detected by the conventional method (Fig. 2). In contrast, the control antibody, which was a larger protein (25 kDa) than the peptide samples (2-4 kDa), was clearly detected at almost the same intensity by both methods (Fig. 2B). Although I used a PVDF membrane with a 0.2 μm pore size, which is well-suited for detecting proteins or peptides of a molecular weight less than 20 kDa, I could not detect three peptides by the conventional method. This is probably because small peptides tend to detach from the blotted membrane more easily than the control antibody.

Tween 20 is frequently used in Western blotting to reduce non-specific binding and background signals. However, a previous study showed that Tween 20 dissociates bound proteins from the nitrocellulose membrane [9]. To further elucidate the reasons why some peptides cannot be detected in the conventional method, I evaluated the effect of Tween 20 on peptide detachment from the blotted membrane. Because CP1 was not detected by the conventional method, I chose CP1 as the model peptide that easily detaches from the membrane in the conventional method. Initially, I detected CP1 by the vacuum method and then I subjected the membrane to repeated 10-min washings with TBS-T or TBS using gentle shaking. After the fourth washing with TBS-T, the observed intensity was decreased to 6.3% of its original value (Fig. 3). Similarly, the intensity declined by 18.2% of its original value after the fourth washing with TBS. These results suggested that peptide detachment was mainly induced by washing with gentle shaking. Moreover, I clearly confirmed that detachment of the peptides from the membrane was accelerated in the presence of Tween 20. Therefore, the decrease of the peptide intensity was inevitable in the conventional method.

3-5 Discussion

I speculated that peptide detachment occurs during washing of the membrane in the conventional method, even if the shaking is done gently. Moreover, the membrane is also shaken gently during the blocking and incubation steps in the conventional method. These gentle shakings may induce peptide detachment from the blotted membrane. Because I used SA-HRP to detect the biotinylated protein and peptides directly, only three washing steps were needed. However, when primary and secondary antibodies are used to detect the protein and peptides, the number of washing and incubation steps increases. Accordingly, it is probable that more peptide detachment occurs when using a primary and secondary antibody. On the other hand, in the case of the vacuum-assisted detection method, there is no need for shaking during any of the immunodetection steps. I think this is the reason why I could detect small peptides sensitively by the vacuum method only.

I could not find correlation between the retention of peptides on the membrane and the properties of the peptides (Mw, pI, GRAVY score, Table 1). Interestingly, the three cysteine-containing peptides, TEWP, pBD2, and TPI, could be detected by the conventional method, although their intensities were weak. Taking this characteristic into account, I think that the three peptides detectable by the conventional method may form intermolecular disulfide bridges. Although the tricine-SDS-polyacrylamide gel electrophoresis was performed under a reducing condition, it is possible that the cysteines in the peptides form intermolecular disulfide bridges through subsequent steps. Therefore, their retention on the membrane may be improved by intermolecular disulfide bridges. It seems likely that the formation of intermolecular disulfide bridges and the fixation with aldehyde have similar effects on the retention of peptides on the PVDF membrane.

At the present time, the fixation of blotted membranes with aldehyde is widely used to

detect small proteins and peptides. However, because previous studies suggest that fixation with aldehyde affects the immunoreactivity of proteins, it is not the best way to improve peptide retention. In this study, I succeeded in detecting small peptides sensitively and clearly using the vacuum-assisted detection method without the need for fixation of the blotted membranes. The vacuum method will enable us to detect previously undetectable proteins and peptides that easily detach from the blotted membranes. In the near future, the vacuum method will be an indispensable tool for sensitive detection and accurate quantification of low-molecular-weight peptides

3-6 References

[1] N. Nishi, M Inui, H. Miyanaka, H. Oya, F. Wada, Western Blot Analysis of Epidermal Growth Factor Using Gelatin-Coated Polyvinylidene Difluoride Membranes, Anal. Biochem. 227 (1995) 401-402.

[2] Y. Suzuki, Y. Takeda, T. Ikuta, Immunoblotting conditions for human hemoglobin chains, Anal. Biochem. 378 (2008) 218-220.

[3] B.R. Lee, T. Kamitani, Improved Immunodetection of Endogenous α-Synuclein, PLoS one 6 (2011) e23939.

[4] B.M. Riederer, Antigen Preservation Tests for Immunocytochemical Detection of Cytoskeletal Proteins: Influence of Aldehyde Fixatives, J. Histochem. Cytochem. 37 (1989) 675-681.

[5] H. Schägger, Tricine-SDS-PAGE, Nature Protocols 1 (2006) 16-22.

[6] K. Fujimoto, T. Ueno, N. Nagata, K. Kashiwagi, K. Aritake, F. Amano, Y. Urade, Suppression of Adipocyte Differentiation by Aldo-keto Reductase 1B3 Acting as Prostaglandin F2α Synthase, J. Biol. Chem. 285 (2010) 8880-8886.

[7] D.J. Kennedy, S. Kuchibhotla, K.M. Westfall, R.L. Silverstein, R.E. Morton, M. Febbraio, ACD36-dependent pathway enhances macrophage and adipose tissue inflammation and impairs insulin signalling, Cardiovasc. Res. 89 (2011) 604-613.

[8] T.N. Tran, S.H. Kim, C. Gallo, M. Amaya, J. Kyees, V. Narayanaswami, Biochemical and biophysical characterization of recombinant rat apolipoprotein E: Similarities to human apolipoprotein E3, Arch. Biochem. Biophys. 529 (2013) 18-25.

[9] W.L. Hoffman, A.A. Jump, Tween 20 removes antibodies and other proteins from nitrocellulose, J. Immunol. Methods 94 (1986) 191-196.

Table 1. Amino acid sequences and properties of the peptides used in this study

Name	Amino acid sequence[a]	Number of cysteines	Mw	pI	GRAVY score[b]
Turtle Egg-White Protein (TEWP)	EKKCPGRCTL KCGKHERPTL PYNCGKYICC VPVKVK	6	4080.9	9.4	-0.608
porcine β-Defensin 2 (pBD2)	DHYICAKKGG TCNFSPCPLF NRIEGTCYSG KAKCCIR	6	4085.7	8.9	-0.289
Tachyplesin I (TPI)	KWCFRVCYRG ICYRRCR	4	2268.7	9.9	-0.518
Bobinin-Like Peptide 7 (BLP7)	GIGGALLSAG KSALKGLAKG LAEHFAN	0	2551.9	9.7	0.415
Magainin 2 (MG2)	GIGKFLHSAK KFGKAFVGEI MNS	0	2466.9	10.0	0.083
Cecropin P1 (CP1)	SWLSKTAKKL ENSAKKRISE GIAIAIQGGP R	0	3338.9	10.6	-0.558

a. All peptides are C-terminally biotinylated.

b. GRAVY stands for grand average of hydropathy. The Positive GRAVY scores indicate hydrophobic peptides, and negative scores indicate hydrophilic peptides.

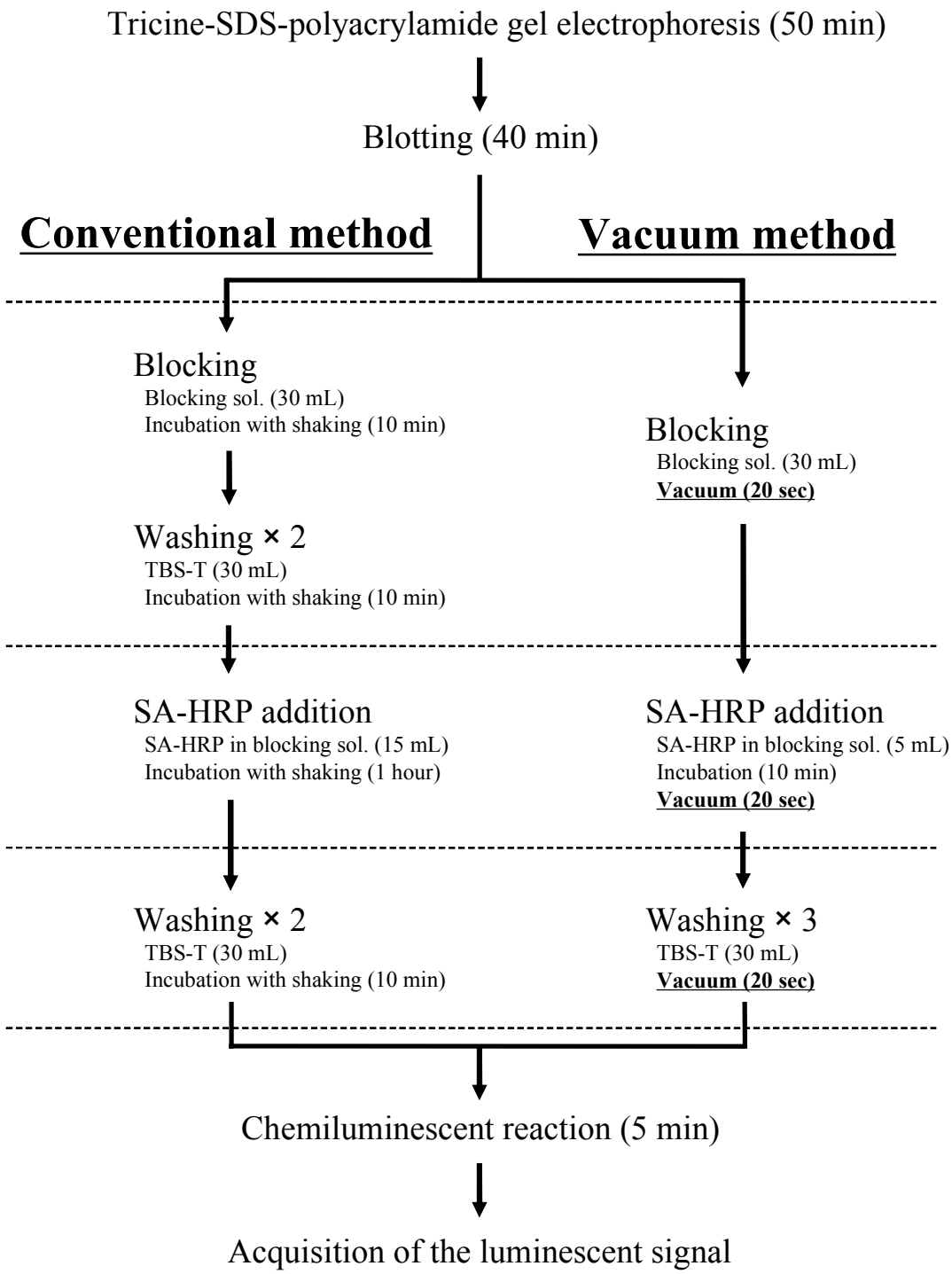

Figure 1. Comparison of the conventional method and the vacuum method. Flowchart of the conventional method (left) and the vacuum method (right). This figure shows solution volume and time required for each step.

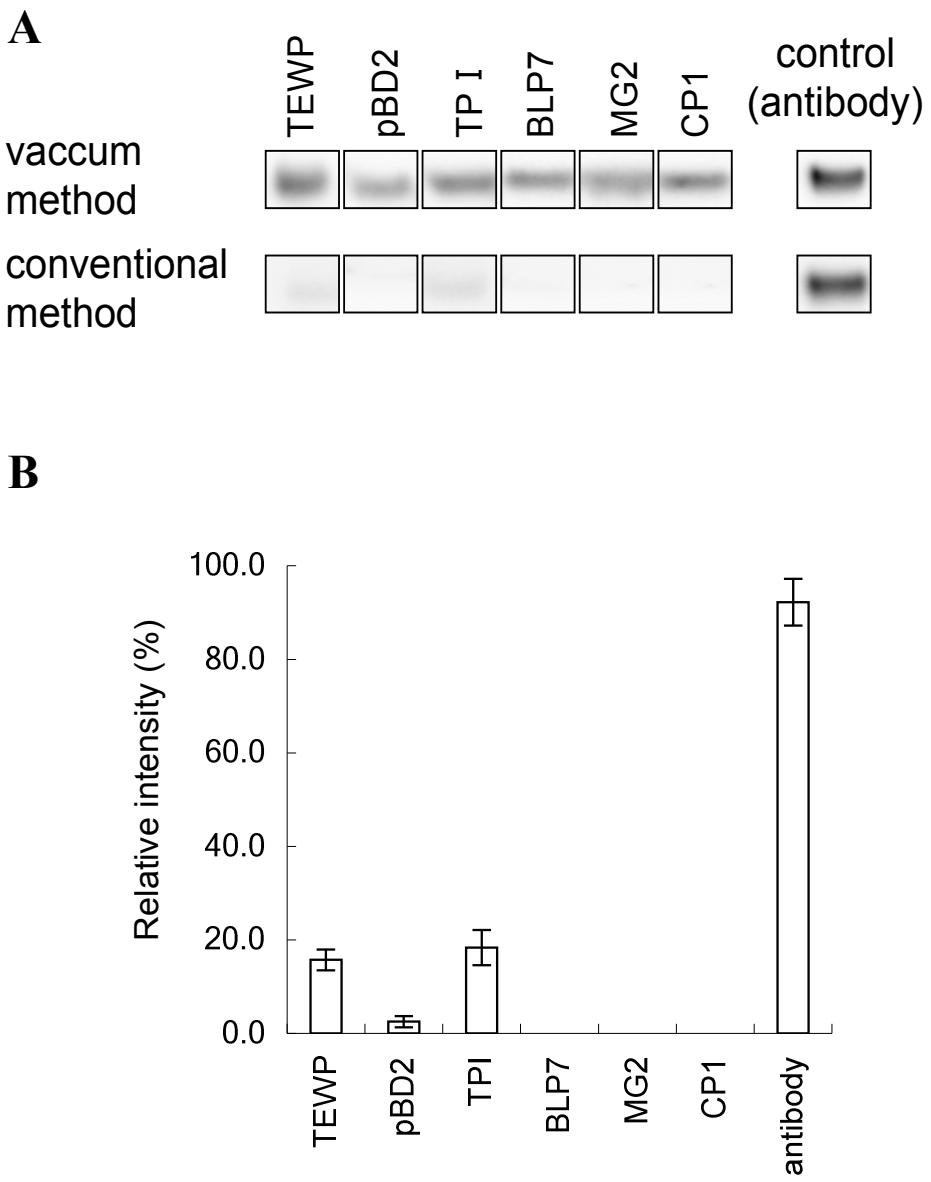

Figure 2. Effectiveness of the use of the vacuum method in Western blotting analysis of small peptides. (A) Comparison of the vacuum method (upper panel) and the conventional method (lower panel). Equimolar amounts (0.2 pmol) of the six peptides were electrophoresed and electrotransferred. A biotinylated antibody was used as a positive control in Western blotting analysis. The luminescent signals were acquired for 120 s by using a cooled CCD camera system. The experiment was conducted three times. (B) The intensity data of the conventional method were expressed in relation to those for the vacuum method.

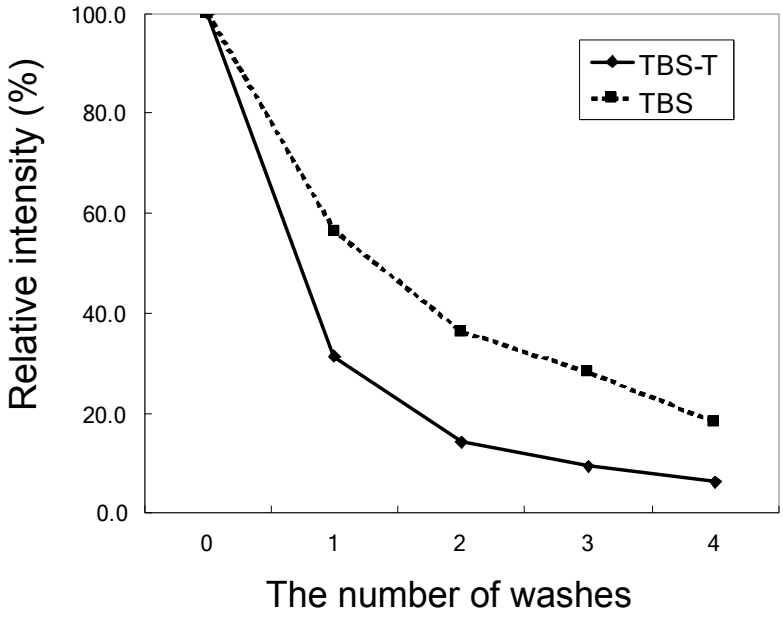

Figure 3. Effect of washing on peptide retention. Comparison of the effects of washing with TBS-T (solid line) and with TBS (dotted line). The intensity of each step was expressed in relation to the original value.

Acknowledgements

I gratefully acknowledge the invaluable suggestions and support of Professor Keiichi Kawano and Associate Professor Tomoyasu Aizawa. I would also like to express my gratitude to Professor Makoto Demura, Lecturer Takashi Kikukawa, Assistant Professor Masakatsu Kamiya and Dr. Yasuhiro Kumaki for their fruitful suggestions and support.